BIOCHEMISTRY
including biophysical chemistry & molecular biology

Article

pubs.acs.org/biochemistry

Hemoglobin Bohr Effects: Atomic Origin of the Histidine Residue Contributions

Guishan Zheng,[‡] Michael Schaefer,[§] and Martin Karplus*[,‡,∥]

[‡]Department of Chemistry and Chemical Biology, Harvard University, Cambridge, Massachusetts 02138, United States
[§]Novartis Institutes for BioMedical Research, Klybeckstrasse 141, 4053 Basel, Switzerland
[∥]Laboratoire de Chimie Biophysique, ISIS Universite de Strasbourg, 67000 Strasbourg, France

Supporting Information

ABSTRACT: The Bohr effect in hemoglobin, which refers to the dependence of the oxygen affinity on the pH, plays an important role in its cooperativity and physiological function. The dominant contribution to the Bohr effect arises from the difference in the pK_a values of His residues of the unliganded (deoxy) and liganded (carbonmonoxy) structures. Using recent high resolution structures, the residue pK_a values corresponding to the two structures are calculated. The method is based on determining the electrostatic interactions between residues in the protein, relative to those of the residue in solution, by use of the linearized finite difference Poisson−Boltzmann equation and Monte Carlo sampling of protonation states. Given that good agreement is obtained with the available experimental values for the contribution of His residues in HbA to the Bohr effect, the calculated results are used to determine the atomic origin of the pK_a shift between deoxy and carbonmonoxy HbA. The contributions to the pK_a shift calculated by means of the linear response approximation show that the salt bridge involving His146 plays an important role in the alkaline Bohr effect, as suggested by Perutz but that other interactions are significant as well. A corresponding analysis is made for the contribution of His143 to the acid Bohr effect for which there is no proposed explanation. The method used is summarized and the program by which it is implemented is described in the Appendix.

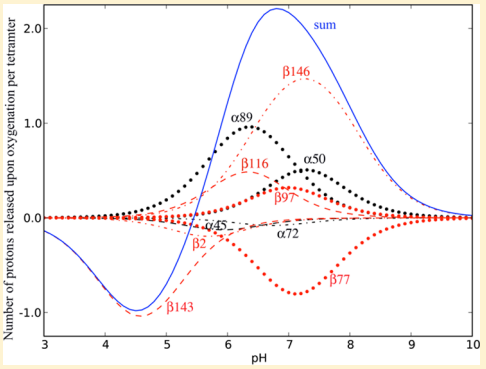

INTRODUCTION

Hemoglobin is the paradigmatic molecule for studies of cooperativity in proteins.[1] The dependence of the oxygen affinity on the hydrogen ion concentration, the Bohr effect, plays an important role in its cooperativity and physiological function. It is named after Christian Bohr, the father of Niels Bohr, who showed in 1904 that increasing the CO_2 concentration decreased the oxygen affinity of dog blood.[2,3] Although Bohr recognized the importance of the effect for efficient oxygen transport by hemoglobin from the lungs to the tissues, he actually never mentioned pH nor the change in protonation state. Bohr and his student Krogh also found by careful measurements that the oxygen binding curve was sigmoidal, an early indication of cooperativity. According to Edsall's review,[4] it was Haldane and collaborators,[5] who in 1914 first proposed that "one or more acidic groups in the hemoglobin molecule became more strongly acidic when oxygen was bound to the iron". Another interesting historical account describes the focus of Wyman and co-workers on Histidine (His) residues as the Bohr groups prior to any structural data.[6] Mutation and chemical modification studies also suggested that the titration of histidines, particularly His β146, was involved,[1,7−9] but it was not until X-ray structures were determined by Perutz and his co-workers for unliganded (deoxy) and liganded (oxy; actually met) hemoglobin that an atomic interpretation was suggested.

In a now famous paper,[10,11] Perutz proposed a mechanism that explained both cooperativity and the Bohr effect in terms of a small number of amino acids, which had different interactions with the rest of the protein in deoxy and oxy Hb; these groups form salt bridges in deoxy Hb that are broken in oxy Hb. Perutz's schematic proposal was made quantitative by a thermodynamic codification which was developed shortly thereafter.[12,13] The model, referred to as the Szabo-Karplus model (SK), encompasses the Monod, Wyman, Changeux (MWC) formulation[14] of cooperativity and, therefore, provides a structural interpretation of it. The SK model has a set of physically meaningful parameters, which when refined by fitting to the relatively precise experimental data of Roughton and Lister[15] gives a quantitative description of hemoglobin cooperativity and the Bohr effect. One striking result from the SK model, which is implicit in the Perutz scheme, is that the Hill cooperativity parameter "n" varies with pH, in disagreement with the dogma that was accepted at the time the model was published. In the model, the Bohr effect arises from the pK_a change of His β146 and Val α1 of the beta and alpha chains, respectively, as a result of the breaking of six salt bridges due to

Received: August 16, 2013
Revised: October 11, 2013
Published: November 13, 2013

   dx.doi.org/10.1021/bi401126z | *Biochemistry* 2013, 52, 8539−8555

tertiary and quaternary structural changes on oxygenation; recognition of the importance of the tertiary changes goes beyond the classic MWC model, though it was considered in the discussion section of the 1965 paper.

Over the years, new data have led to refinements of the SK model by a number of workers.[16−18] Moreover, two types of concerns have been raised with respect to the Perutz model of the alkaline Bohr effect and its thermodynamic interpretation. The first question whether ascribing the alkaline Bohr effect to the Perutz salt bridges is a complete description; i.e., it was suggested that other amino acids contribute as well.[19] The second is whether the specific salt bridges suggested by Perutz or more delocalized interactions are the main factor in altering the pK_a's of the Bohr groups between the deoxy and oxy Hb structure.

It is only relatively recently that advances of NMR spectroscopy and its application to hemoglobin by Ho and his co-workers have confirmed that His β146 is a dominant contributor to the Bohr effect.[19,20] They were able to measure the pK_a's in deoxy and carbonmonoxy hemoglobin for 24 out of the total of 36 His in HbA, and to show that the pK_a difference between the deoxy and oxy structures provides an explanation of about 86% of the alkaline Bohr effect at pH 7.4. Specifically, they answered the first question, i.e., His β146 makes the most important contribution to the alkaline Bohr effect, but other His contribute as well.

To further our understanding of the origin of dominant contributions to the Bohr effect and to answer the second question, we present a computational study that focuses primarily, though not entirely, on the pK_a values of the His residues in deoxy and oxy hemoglobin. In addition, we examine all other titratable residues to determine whether they can contribute to the Bohr effect. Since Ho et al. did their NMR measurements on stripped (no allosteric effectors) deoxy (HbA) and carbonmonoxy hemoglobin (CO HbA), we chose to study these species, which makes possible the most direct comparison with their measurements. We determine the role of the salt bridges proposed by Perutz as shifting the pK_a values by estimating all the interactions that make significant contributions. Our analysis focuses particularly on the deoxy structure, which has the larger pK_a shifts, and on residues His β146 and His β143, which make the largest contribution to the alkaline and acid Bohr effect, respectively.

Since the dominant contributions to pK_a shifts have been shown to arise from electrostatic interactions,[21−25] we use the linearized finite-difference Poisson−Boltzmann equation (PB) for the calculations. It has been shown to give quantitative results for the pK_a shifts in proteins relative to model compounds in solution in many applications.[25,26] Although free energy simulations[27−29] and constant pH molecular dynamics methods[30−32] could be used, the PB approach has the advantage, important for a molecule as large as hemoglobin, that it requires much less computer time and that the decomposition of the pK_a shift into individual contributions from protein residues is relatively straightforward. As noted by Bashford et al. for myoglobin,[23] the calculated pK_a values vary with the structure used, so an important element in any PB calculation is the atomic structure on which it is based. There are a number of relatively high resolution X-ray structures for hemoglobin, both unliganded and liganded (with O_2 and CO) (see Table 1). This makes it possible to apply the PB method to the various structures and determine the range of results. For unliganded Hb, the structures are relatively similar. For the liganded state, the available structures differ significantly and there is considerable controversy as to which structure or combination of them corresponds to the solution ensemble in the NMR measurements.[19,20] By employing the present approach, we obtain some insights into this question.

Table 1. Deoxy- and Oxy-Hemoglobin Crystal Structures

ligation state	PDB ID	resolution (Å)	reference
Deoxy	2DN2	1.25	45
	4HHB	1.74	56
	1BZ0	1.50	57
	1KD2	1.87	unpublished
	1RQ3	1.91	58
	1XXT	1.91	59
Oxy	2DN3	1.25	45
	1HHO	2.10	46
	1BBB	1.70	47
	1MKO	2.18	48
	1YZI	2.07	48

The only earlier computational studies that we could find concerned with the Bohr effect are one based on the Tanford-Kirkwood spherical electrostatic model with parameters adjusted to obtain approximate agreement with available experimental data,[33] although the correct assignments of individual His residues were not available, and another,[34] which is a predecessor of the present work; it used the original Bashford-Karplus model, lower resolution structures of HbA, and the CHARMM 22 force field.

The method section presents a summary of the PB method, which is based on Schaefer et al.[26] The next section describes the results. It lists the X-ray structures for unliganded and liganded HbA that we consider. A description is given for the structure used for the pK_a calculations, which were prepared from the X-ray structures by minimization and application of the WHATIF program.[35] The calculated pK_a values, pK_a^{eff}, of the His residues are then compared with the experimental values. Examples of the sensitivity of the calculated results to the choice of structure are presented. Given that the calculations yield essentially correct values for the measured His pK_a's of unliganded and liganded HbA if high-resolution structures are employed, we use the values to calculate the His contribution to the alkaline and acids Bohr effects and compare the results with the experimental values. For His β146 and His β143, which are most important for the alkaline and acid Bohr effect, respectively, the electrostatic interaction energies and a perturbation approximation are then used to analyze the pK_a shift from pK_a^{stnd}, the pK_a value of the model compound in solution, to pK_a^{eff}, the corresponding pK_a value in the protein. A concluding discussion is given at the end.

METHODOLOGY AND COMPUTATIONAL DETAILS

By definition, the effective pK_a of a titratable residue is equal to the pH at which the protonated and unprotonated states are occupied with 50% probability. Calculating the effective pK_a's for a protein of known structure thus requires computing the average protonation state of each titrating residue as a function of pH. In what follows, it is assumed that the free energy that determines the protonation state of a titratable residue in a protein is of electrostatic origin and that the linearized finite difference Poisson−Boltzmann equation is applicable. We use the generalized formulation developed by Schaefer et al.,[26] based on the earlier work of Bashford and Karplus.[21,36] The former is employed because it provides a consistent method for treating titratable residues with more than two charge states,

dx.doi.org/10.1021/bi401126z | Biochemistry 2013, 52, 8539−8555

as is required for histidine side chains. The actual program used for the calculations is described in the Appendix.

Theory. The protein is considered to be composed of N titratable atomic groups (generally side chains), and the nontitrating "background" atomic groups, where the latter includes both backbone atoms, and the side chain atoms whose charges are unchanged during titration, independent of pH. The need for doing quantum mechanical calculations[22] is avoided by calculating pK_a-changes relative to the known standard pK_a of a titrating amino acid residue in solution.

Following Schaefer et al.[26] with slight modification, the electrostatic free energy at a given pH for a protein with N titratable residues in a given protonation state, relative to the system where all titrating groups have zero net charge, is given by

$$\Delta G(\mathbf{s}, pH) = E(\mathbf{s}) - E(\mathbf{0}) - [E^M(\mathbf{s}) - E^M(\mathbf{0})] + (\ln 10)k_BT\sum_{i=1}^{N}[n(s_i)\mathrm{pH} - \mathrm{p}K_{a,i}^{\mathrm{stnd}}(s_i)] \quad (1a)$$

$$= (\ln 10)k_BT\sum_{i=1}^{N}[n(s_i)\mathrm{pH} - \mathrm{p}K_{a,i}^{\mathrm{stnd}}(s_i)] + \sum_{i>j=1}^{N}[E_{ij}(s_i, s_j) - E_{ij}(s_i^0, s_j^0)] + \sum_{i=1}^{N}[E_{i0}(s_i) - E_{i0}(s_i^0)] + \sum_{i=1}^{N}[E_{ii}(s_i, s_i) - E_{ii}(s_i^0, s_i^0)] - \sum_{i=1}^{N}[E_{i0}^{M_i}(s_i) - E_{i0}^{M_i}(s_i^0)] - \sum_{i=1}^{N}[E_{ii}^{M_i}(s_i, s_i) - E_{ii}^{M_i}(s_i^0, s_i^0)] \quad (1b)$$

$$= (\ln 10)k_BT\sum_{i=1}^{N}[n(s_i)\mathrm{pH} - \mathrm{p}K_{a,i}^{\mathrm{stnd}}(s_i)] + E_{\mathrm{inter}} + E_{\mathrm{back}} + E_{\mathrm{Born}} - E_{\mathrm{back}}^M - E_{\mathrm{Born}}^M \quad (1c)$$

In eq 1, the protonation state vector $\mathbf{s} = (s_1, s_2, ..., s_N)$ has components s_i which give the protonation state index of residue i. The component s_i^0 is the reference protonation state index for site i; in practice, s_i^0 is chosen as a protonation state of the side chains with zero net charge (see the section Computational Details). For a residue with two states, s_i is

$$s_i = \begin{cases} 0, & \text{unprotonated state} \\ 1, & \text{protonated state} \end{cases} \quad (2)$$

For a His residue, there are three protonation states: the protonated His (His^+ with hydrogens on both N^ε and N^δ) and the two unprotonated states with a hydrogen on N^ε *or* N^δ. The neutral charge state with N^δ protonated is chosen as $s_i = 0$, the state with N^ε protonated as $s_i = 1$ and His^+ as $s_i = 2$. For His residues, N^δ is chosen arbitrarily as the reference state, even though N^ε has been shown to be of lower free energy than N^δ; the concentration ratio ε:δ is 70:30 in solution.[37] The choice of the reference state is made for convenience and the final pK_a values are independent of this choice.

The number of protons on the residue i with index s_i is given by $n(s_i)$. For a residue with two states, $n(s_i) = s_i$ and, according to the convention for His in the previous paragraph, $n(s_i)$ is given by

$$n(s_i) = \begin{cases} 0, & s_i = 0 \quad (N^\delta) \\ 0, & s_i = 1 \quad (N^\varepsilon) \\ 1, & s_i = 2 \quad (His^+) \end{cases} \quad (3)$$

In eq 1, $E(\mathbf{s})$ is the total electrostatic free energy of the protein in state s and $E(\mathbf{0})$ is the total electrostatic free energy of the reference protonation state, where all titratable sites are in their charge neutral states as noted above. Corresponding definitions hold for the free energies of the model compounds, $E^M(\mathbf{s})$ and $E^M(\mathbf{0})$. The terms $E(\mathbf{s})$-$E(\mathbf{0})$ and $E^M(\mathbf{s})$-$E^M(\mathbf{0})$ are written out in eq 1b and related to certain definitions in eq 1c. Comparing eq 1b and eq 1c, we have in the protein environment, E_{inter}, the electrostatic interaction energy between titratable residues:

$$E_{\mathrm{inter}} = \frac{1}{2}\sum_{i\neq j=1}^{N}[E_{ij}(s_i, s_j) - E_{ij}(s_i^0, s_j^0)] \quad (4a)$$

E_{back}, the electrostatic interaction energy between the titratable residues and background atoms:

$$E_{\mathrm{back}} = \sum_{i=1}^{N}[E_{i0}(s_i) - E_{i0}(s_i^0)] \quad (4b)$$

and E_{Born}, the Born energy:

$$E_{\mathrm{Born}} = \sum_{i=1}^{N}[E_{ii}(s_i, s_i) - E_{ii}(s_i^0, s_i^0)] \quad (4c)$$

All of these are given relative to the reference protonation state. Correspondingly, for the model compounds, we have

$$E_{\mathrm{back}}^M = \sum_{i=1}^{N}[E_{i0}^{M_i}(s_i) - E_{i0}^{M_i}(s_i^0)] \quad (4d)$$

and

$$E_{\mathrm{Born}}^M = \sum_{i=1}^{N}[E_{ii}^{M_i}(s_i, s_i) - E_{ii}^{M_i}(s_i^0, s_i^0)] \quad (4e)$$

with there being no interaction term.

In eq 4a, E_{inter} consists of $E_{ij}(s_i, s_j)$, the electrostatic interaction free energy between residue i and residue j in states i and j minus $E_{ij}(s_i^0, s_j^0)$, that in the reference states. The quantity E_{back} (eq 4b) is a sum over each titratable residue in state s_i interacting with all background atoms (indicated by the subscript 0) minus the corresponding term for the reference state. The terms E_{back}^M (eq 4d) and E_{Born}^M (eq 4e) are the corresponding contributions in the model compound. Given eq 1a, it is necessary to find the value of $\Delta G(\mathbf{s}, \mathrm{pH})$ that minimizes the total electrostatic free energy as a function of all possible values of s_i; a Monte Carlo procedure is used when the number of titratable residues is large (see below). We remind the reader that for each residue i, only one of the possible protonation states appears in eq 1a, as indicated by the value of s_i.

The average protonation state of the protein as a function pH, $\bar{\mathbf{n}}(\mathrm{pH})$ is determined from $\Delta G(\mathbf{s}, \mathrm{pH})$ using the statistical mechanical average

dx.doi.org/10.1021/bi401126z | *Biochemistry* 2013, 52, 8539−8555

Table 2. Root Mean Square Difference (Heavy Atoms Only) Between Hemoglobin Crystal Structures in Å

	deoxy							oxy				
PDB ID	2DN2	4HHB	1BZ0	1HGA	1RQ3	1XXT	1KD2	2DN3	1HHO	1BBB	1MKO	1YZI
2DN2												
4HHB	0.55											
1BZ0	0.69	0.69										
1HGA	0.95	0.94	0.83									
1RQ3	0.83	0.84	0.72	0.76								
1XXT	0.77	0.77	0.8	0.86	0.56							
1KD2	0.81	0.75	0.83	0.9	0.83	0.75						
2DN3	2.77	2.79	2.81	2.93	2.95	2.93	2.99					
1HHO	2.65	2.67	2.69	2.82	2.83	2.82	2.87	1.47				
1BBB	3.84	3.86	3.84	4.04	4.03	4.05	4.07	2.18	2.23			
1MKO	3.44	3.45	3.45	3.6	3.6	3.62	3.66	1.72	1.91	1.39		
1YZI	3.98	3.99	4.02	4.09	4.16	4.14	4.2	2.28	2.09	3.03	2.53	

Table 3. Root Mean Square Difference (Heavy Atoms only) (Å) between Hemoglobin Minimized WHATIF Structures

	deoxy						oxy				
PDB ID	2DN2	4HHB	1BZ0	1RQ3	1XXT	1KD2	2DN3	1HHO(R)	1BBB(R2)	1MKO(RR2)	1YZI(R3)
min vs unmin.	0.68	0.70	0.67	0.72	0.68	0.70	0.68	0.88	0.73	0.82	0.77
2DN2											
4HHB	0.61										
1BZ0	0.68	0.62									
1RQ3	0.86	0.82	0.84								
1XXT	0.87	0.82	0.83	0.50							
1KD2	0.89	0.82	0.81	0.84	0.82						
2DN3	2.85	2.84	2.88	2.98	2.98	3.06					
1HHO	2.71	2.71	2.74	2.85	2.85	2.92	1.53				
1BBB	3.87	3.85	3.88	4.04	4.05	4.08	2.20	2.26			
1MKO	3.48	3.47	3.52	3.65	3.66	3.71	1.71	1.96	1.44		
1YZI	3.97	3.96	4.01	4.11	4.10	4.17	2.21	2.08	2.98	2.49	

Table 4. Deoxy His pK_a Values and Absolute Deviations (Numbers in Parentheses) From Experimental Values Using Minimized WHATIF Structures

Subunit	ResID	NMR	**2DN2**	4HHB	1BZ0	1RQ3	1XXT	1KD2
α	20	7.02	**6.14 [0.88]**	7.11 [0.09]	6.93 [0.09]	6.95 [0.07]	6.95 [0.07]	6.78 [0.24]
α	45	5.25	**5.88 [0.63]**	5.90 [0.65]	5.85 [0.60]	5.64 [0.39]	5.56 [0.31]	6.01 [0.76]
α	50	7.14	**7.50 [0.36]**	7.35 [0.21]	7.30 [0.16]	7.15 [0.00]	7.21 [0.07]	7.05 [0.09]
α	58		**4.33**	4.54	4.06	3.54	3.79	4.55
α	72	7.47	**6.69 [0.78]**	6.67 [0.80]	6.72 [0.75]	6.89 [0.59]	6.74 [0.73]	6.68 [0.80]
α	87		**2.95**	3.05	3.28	3.45	3.89	3.43
α	89	6.80	**6.82 [0.02]**	6.78 [0.02]	6.46 [0.34]	6.82 [0.02]	6.77 [0.03]	6.54 [0.26]
α	103		**3.92**	4.19	3.58	3.60	3.55	4.37
α	112	7.49	**6.64 [0.85]**	6.93 [0.56]	6.66 [0.83]	6.60 [0.89]	6.89 [0.60]	6.84 [0.65]
α	122		**0.53**	0.64	0.78	0.99	0.82	1.08
β	2	6.17	**5.61 [0.56]**	5.51 [0.66]	5.27 [0.90]	4.97 [1.20]	5.12 [1.05]	5.70 [0.47]
β	63		**4.93**	5.30	4.84	5.69	4.82	3.85
β	77	7.46	**6.76 [0.70]**	6.70 [0.76]	6.89 [0.57]	6.92 [0.54]	6.83 [0.63]	7.05 [0.41]
β	92		**3.61**	3.70	3.56	3.22	3.14	3.73
β	97	8.01	**7.13 [0.88]**	7.26 [0.75]	7.02 [0.99]	7.12 [0.89]	7.04 [0.97]	7.04 [0.97]
β	116	6.35	**6.55 [0.20]**	6.64 [0.29]	6.36 [0.01]	5.71 [0.64]	5.62 [0.73]	6.74 [0.39]
β	117	6.43	**8.01 [1.58]**	8.11 [1.68]	7.44 [1.01]	7.57 [1.14]	7.77 [1.34]	6.28 [0.15]
β	143	4.70	**4.08 [0.62]**	3.85 [0.85]	4.52 [0.19]	4.82 [0.12]	4.69 [0.02]	4.82 [0.12]
β	146	7.93	**8.08 [0.15]**	7.58 [0.35]	7.86 [0.07]	7.84 [0.09]	7.81 [0.12]	8.12 [0.19]
	Max error		[1.58]	[1.68]	[1.01]	[1.20]	[1.34]	[0.97]
	Ave. error		[0.63]	[0.59]	[0.50]	[0.51]	[0.51]	[0.42]

dx.doi.org/10.1021/bi401126z | *Biochemistry* 2013, 52, 8539−8555

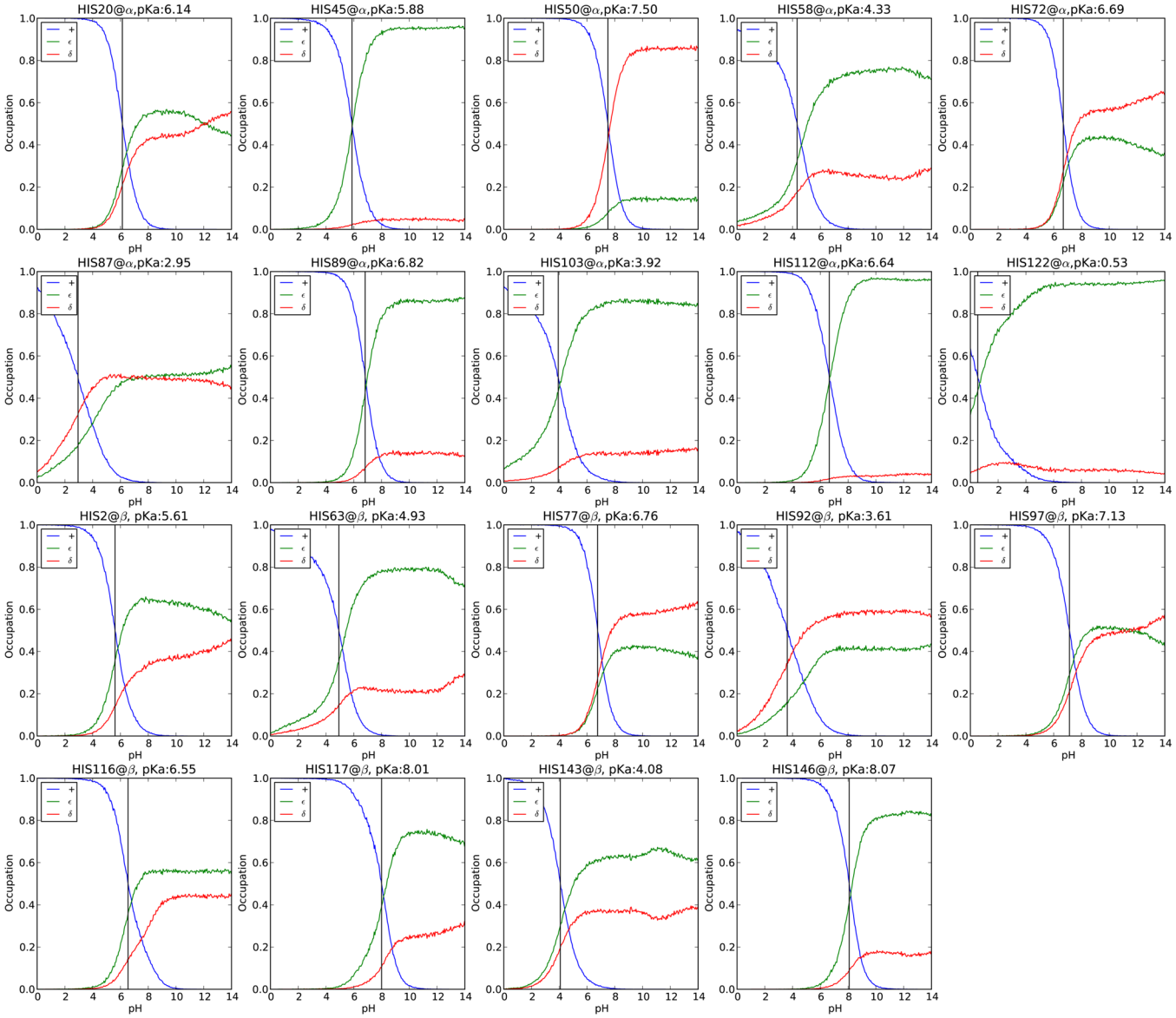

Figure 1. Titration curves of all His residues of 2DN2 (Deoxy). The symbol "+" refers to the "His^+" state, "ε" to N^{ε}, "δ" to N^{δ}. The black line corresponds to the pK_a^{eff} value.

$$\bar{\mathbf{n}}(\mathrm{pH}) = \frac{\sum_{\{\mathbf{s}\}} \mathbf{n}(\mathbf{s}) e^{-\beta \Delta G(\mathbf{s},\mathrm{pH})}}{\sum_{\{\mathbf{s}\}} e^{-\beta \Delta G(\mathbf{s},\mathrm{pH})}} \tag{5}$$

In addition, we calculate $P(s_i', \mathrm{pH})$, the probability (average occupancy) of each protonation state s_i at titrating site i at a given pH. It is

$$P(s_i', pH) = \frac{\sum_{\{\mathbf{s}\}} \delta_{s_i s_i'} e^{-\beta \Delta G(\mathbf{s},\mathrm{pH})}}{\sum_{\{\mathbf{s}\}} e^{-\beta \Delta G(\mathbf{s},\mathrm{pH})}} \tag{6}$$

where the Kronecker symbol $\delta_{s_i s_i'}$ is equal to 1 if $s_i = s'_i$ and to 0, otherwise. The quantity β in eq 5 and eq 6 equals $(k_B T)^{-1}$, where k_B is Boltzmann constant and T is the temperature. With the resultant average occupancy of each site for a range of pH values, pK_a^{eff} is obtained as the solution pH when the average protonation state of the residue is equal to half occupancy; if there are three states as in His, half occupancy corresponds to the average occupancy of His^+ state equal to one-half. The value $pK_{a,i}^{stnd}(s_i)$ in eq 1 is defined for sites with only two protonation states, as

$$pK_{a,i}^{stnd}(s_i) = \begin{cases} 0, & \text{if site } i \text{ is unprotonated} \quad (s_i = 0) \\ pK_{a,i}^{stnd}, & \text{if site } i \text{ is protonated} \quad (s_i = 1) \end{cases} \tag{7}$$

where, as defined above, $pK_{a,i}^{stnd}$ is the pK_a of residue i in aqueous solution (see the Computational Details section) for a list of the standard pK_a values). For His, the standard pK_a for the N^{ε} state is 6.53 and for the N^{δ} state is 6.92 from solution measurements. According to the convention (eq 3), the $pK_{a,i}^{stnd}(s_i)$ are

$$pK_{a,i}^{stnd}(s_i) = \begin{cases} 0.00, & s_i = 0 \quad (N^{\delta}) \\ 0.38, & s_i = 1 \quad (N^{\varepsilon}) \\ 6.92, & s_i = 2 \quad (His^+) \end{cases} \tag{8}$$

The intrinsic pK_a, pK_a^{intr}, of a residue in the protein is the pK_a, relative to pK_a^{stnd}, that includes the Born term for the residue in

dx.doi.org/10.1021/bi401126z | Biochemistry 2013, 52, 8539−8555

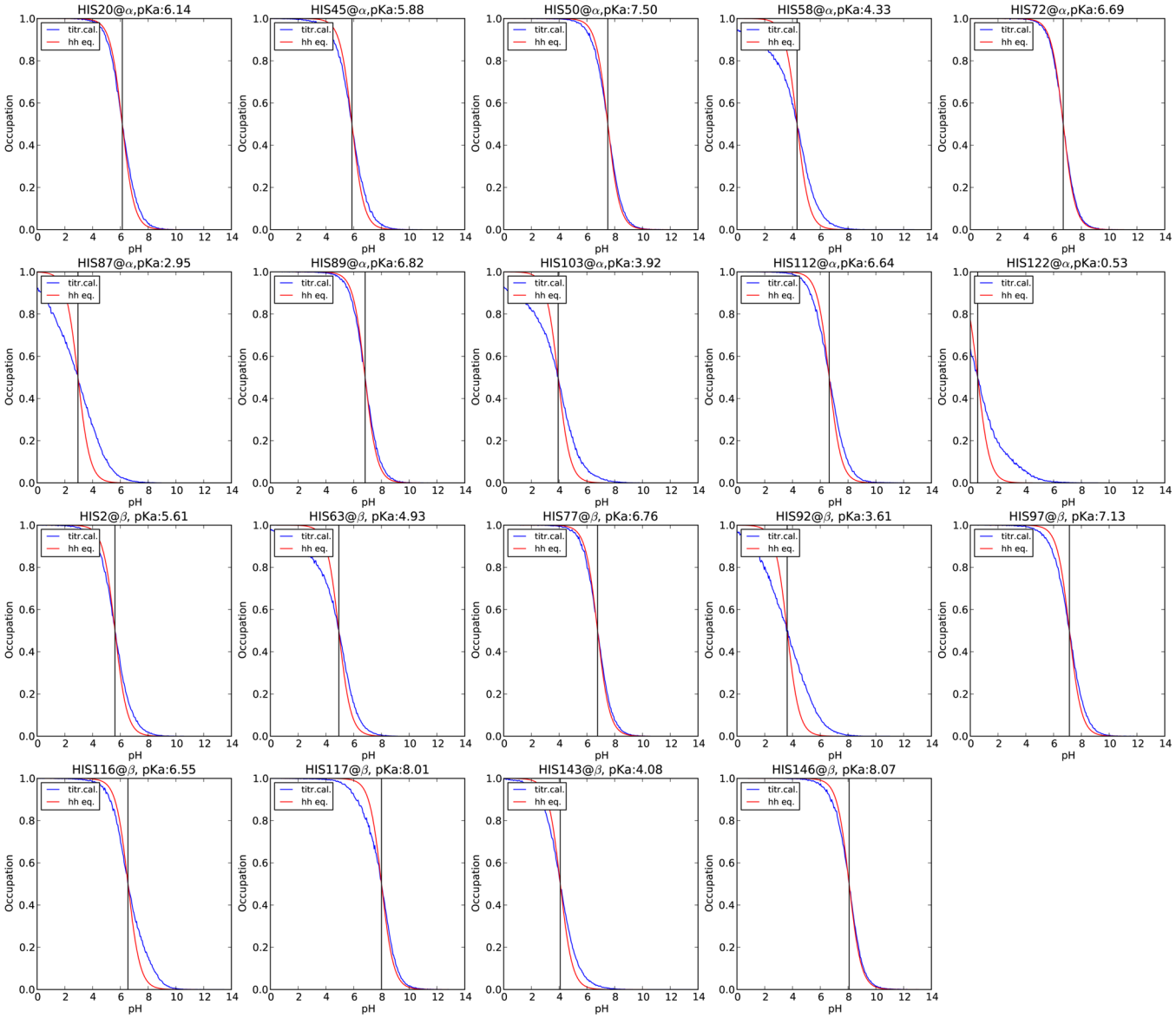

Figure 2. Average protonation curves of His^+ state of all His residues for 2DN2(Deoxy) from titration calculations (titr. cal.) and Henderson–Hasselbalch equation (hh eq.). The black line corresponds to the pK_a^{eff} value.

the protein and its electrostatic interactions with the background atoms. In the CHARMM force field that was used, all side chains have integral charges equal to −1, 0, or +1.

Contributions to pK_a^{eff}. Two approaches were used to obtain information about the origin of the value of pK_a^{eff}, the pK_a of a residue in protein, relative to that of the model compound in solution. Both are approximations to the full calculation. The first is to evaluate each of the terms in eq 4 to determine the Born solvation free energy, the background term, and the interaction energy for the residue with the other titratable residues. The individual values of these terms influence the final average occupancy in an indirect manner since the average occupancy also depends on the ensemble average of all configurations. The second is in the spirit of the first order perturbation theory used previously by one of the authors,[38,39] to find the contribution of individual residues to the free energy along the reaction path of an enzymatic reaction. Here the titratable side chain atoms of a given residue j are deleted and the Monte Carlo sampling of the system is repeated to find the change in the pK_a^{eff} of residue i. The difference between the new pK_a^{eff} value and the original one is considered to be the contribution from residue j to the shift in the pK_a value of residue i. In the present application, as well as in the earlier analysis, the perturbation approach, although approximate, has an advantage over the experimental mutation analysis in that it obtains the contribution in the absence of any structural relaxation induced by the mutation.

COMPUTATIONAL DETAILS

A. Preparation of Structures. The various initial structures for deoxy and oxy HbA were downloaded from www.pdb.org (see Table 1). To correct potential errors in the X-ray structures, e.g., too close nonbonded distances, and to assess the sensitivity of the calculated pK_a^{eff} values to the atomic coordinates, two sets of structures were generated from each of the crystal structures. In one set, the tautomers and protonation states were determined with the WHATIF program,[35] which optimize the hydrogen network. The hydrogen positions in the

dx.doi.org/10.1021/bi401126z | Biochemistry 2013, 52, 8539–8555

Table 5. Oxy HbA His pK_a Values and Deviations (Numbers in Parentheses) From Experimental Values Using Minimized WHATIF Structure

subunit	ResID	oxy(NMR)	**2DN3**	1HHO(R)	1BBB(R2)	1MKO(RR2)	1YZI(R3)
α	20	7.08	**7.15 [0.07]**	7.18 [0.10]	7.05 [0.03]	7.18 [0.10]	7.03 [0.05]
α	45	6.12	**5.99 [0.14]**	5.86 [0.26]	6.14 [0.02]	6.24 [0.12]	6.46 [0.34]
α	50	6.90	**7.05 [0.15]**	7.04 [0.14]	7.40 [0.50]	7.28 [0.38]	7.26 [0.36]
α	58		**3.88**	3.55	5.00	4.40	5.04
α	72	7.27	**6.76 [0.51]**	6.58 [0.69]	6.68 [0.59]	6.82 [0.45]	6.72 [0.55]
α	87		**3.71**	3.16	3.69	3.09	3.01
α	89	6.25	**5.91 [0.34]**	5.92 [0.33]	7.12 [0.87]	5.80 [0.45]	5.67 [0.59]
α	103		**3.17**	2.79	3.99	2.41	3.94
α	112	7.53	**7.20 [0.33]**	5.80 [1.73]	6.24 [1.29]	6.66 [0.87]	6.22 [1.32]
α	122		**0.79**	1.04	0.77	0.19	1.34
β	2	6.39	**5.78 [0.61]**	5.84 [0.55]	5.93 [0.46]	5.99 [0.40]	6.77 [0.38]
β	63		**5.89**	5.70	6.43	5.69	5.62
β	77	7.79	**7.50 [0.29]**	7.33 [0.46]	7.14 [0.65]	7.39 [0.40]	6.25 [1.54]
β	92		**4.58**	4.30	3.53	4.21	5.25
β	97	7.75	**6.85 [0.90]**	7.01 [0.74]	6.77 [0.98]	6.77 [0.98]	7.62 [0.13]
β	116	6.13	**6.12 [0.01]**	6.33 [0.20]	6.73 [0.60]	6.81 [0.68]	7.16 [1.03]
β	117	6.39	**6.35 [0.04]**	6.05 [0.34]	5.87 [0.52]	6.21 [0.18]	6.80 [0.41]
β	143	5.57	**5.08 [0.49]**	4.75 [0.82]	5.43 [0.14]	4.89 [0.68]	2.29 [3.28]
β	146	6.42	**6.45 [0.03]**	2.24 [4.18]	1.30 [5.12]	5.31 [1.11]	4.58 [1.84]
	Max error		[0.90]	[4.18]	[5.12]	[1.11]	[3.28]
	Ave. error		[0.30]	[0.81]	[0.91]	[0.52]	[0.91]

structures were then subjected to 100 steps of the steepest decent minimization, followed by applying the Adapted Basis Newton−Raphson (ABNR) method in CHARMM[40,41] until the gradient was less than 0.01 kcal/mol/Å. The calculations used the default nonbonding interaction parameters in CHARMM parameter set 27,[42] i.e., the nonbonded interaction cutoff distance is 12.0 Å. The resultant structures are referred to as "unminimized" WHATIF structures in the following sections. The "minimized" WHATIF structures are obtained by further minimization of all atoms of the unminimized WHATIF structures for 1000 steps using the ABNR algorithm and a dielectric constant of 4.5 multiplied by the interatom distance; a cutoff nonbonded interaction distance of 8.0 Å was used.[26] In addition, "unminimized" and "minimized" crystal structures were obtained following the same procedure without WHATIF optimization. For the latter, the protonation states of the His residues were all set to N^{δ} and the hydrogen positions were determined with the HBUILD module in CHARMM version c36a1. We used the α_1 and β_1 Hb chains in all cases; the results for α_2 and β_2 usually, but not always, differ by small amounts (see SI). The model compounds have the composition [NH•C_{α}R•C═O] and the conformation used in eq 1 for calculating E^{M}_{back} and E^{M}_{Born} is that of the specific residue in the protein, i.e., in the thermodynamic cycle used to determine the pK_a^{eff} relative to the solution value, we assume that the free energy difference between the model compound in the unprotonated and protonated form is the solution value, but calculate the free energy difference between the residue in the protein and the residue in solution using the structure in the protein.

B. Calculation of the pK_a^{eff} Values in the Protein. For calculating the pK_a^{eff} using eq 1 and eq 6, the interaction energy between each pair of titratable residue side chains, between a titratable residue and the background charges (that are fixed during the titration), and the Born solvation energy of each titratable site in the model compound and in the protein environment were determined. All the electrostatic free energy values in eq 1, both in the protein and in the model peptide residues, are computed by solving the linearized finite difference Poisson−Boltzmann equation using UHBD program[43] based on a focusing technique, the details of which are outlined below. A dielectric constant of 80 was used for the solvent and a dielectric constant of 20 was used for the protein and the model compound. All calculations were done with an ionic strength of 0.1 M, a temperature of 298 K, and a Stern (ion exclusion) layer of 2.0 Å. Three focusing grids were used to achieve a final grid spacing of 0.3 Å. The titratable residues with their pK_a values in aqueous solution are Arg (12.48), Asp (4.00), Glu (4.40), His [6.92(N^{ε}),6.52(N^{δ})], Lys (10.79), Tyr (10.13), the C-terminal carboxyl (3.80), and the N-terminal amino group (7.50).[26] All atomic radii were assigned according to the CHARMM Parameter Set 27 and the atomic charges are listed in Table S1 in Supporting Information. The Monte Carlo algorithm by Beroza et al.[44] was used to calculate the average protonation states. At a given pH, the average protonation of the sites was determined by performing 5000 "full MC" equilibration steps followed by 10000 "full MC" steps, where 1 "full MC" step corresponds to N random attempts to change the protonation state of the system (N is the number of titratable sites/residues plus the number of strongly coupled sites, i.e., two sites with interaction energy (E_{ij}) less than −0.5 kcal/mol). The maximal absolute error of all His residue pK_a values is less than 0.04 pK_a unit between using 10000 "full MC" and 80000 "full MC" steps. Thus, 10000 "full MC" steps was considered to be sufficient.

C. Calculation of pK_a^{intr}. The intrinsic pK_a of a residue is defined as its pK_a in the protein environment with all other titratable residues in their neutral charge state (His in δ state). The difference between pK_a^{intr} and pK_a^{stnd} (eq 9a) arises from three terms (see also eq 4): the interaction with other titratable residues (eq 9b), the interaction with background atoms (eq 9c), and the Born energy term (eq 9d); that is,

$$pK^{intr}_{a,i}(s_i) = pK^{stnd}_{a,i}(s_i) - \ln(10)\beta E \quad (9a)$$

dx.doi.org/10.1021/bi401126z | Biochemistry 2013, 52, 8539−8555

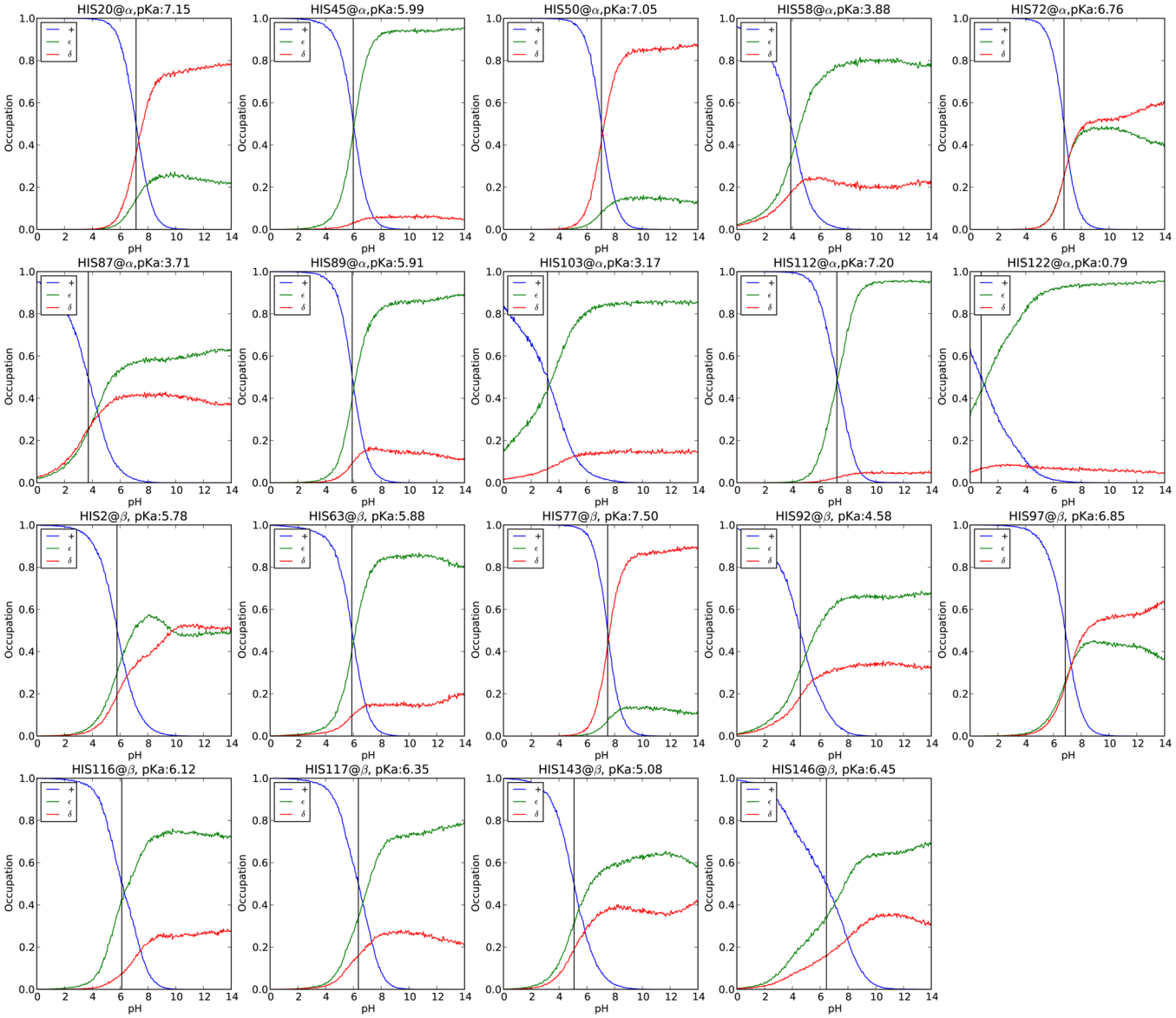

Figure 3. Titration curves of all His residues of 2DN3(Oxy).The symbol ″+″ refers to the ″His^+″ state, ″ε″ to N^{ε}, ″δ″ to N^{δ}. The black line corresponds to the pK_a^{eff} value.

$$E = \sum_{j=1\&j\neq i}^{N} [E_{ij}(s_i, s_j^0) - E_{ij}(s_i^0, s_j^0)] \tag{9b}$$

$$+ [E_{i0}(s_i) - E_{i0}(s_i^0)] - [E_{i0}^{M_i}(s_i) - E_{i0}^{M_i}(s_i^0)] \tag{9c}$$

$$+ [E_{ii}(s_i, s_i) - E_{ii}(s_i^0, s_i^0)] - [E_{ii}^{M_i}(s_i, s_i) - E_{ii}^{M_i}(s_i^0, s_i^0)] \tag{9d}$$

The meanings of the labels can be found in the Theory section. Thus, $pK_{a,i}^{intr}(s_i)$ reflects the desolvation of the sites, i.e., the removal from the solvent and the insertion into the protein.

RESULTS

The primary focus of this paper is on the analysis of the pK_a's of the His residues of deoxy and carbonmonoxy HbA in the absence of other effectors, such as bisphosphoglycerate(BPG). The pK_a's of the surface His are known from the NMR measurements of Ho and co-workers.[19,20] HbA has 38 histidine residues. Each α chain has ten histidine residues and each β chain has nine histidine residues. Of these, six pK_a were measured for each of the α chains and seven for each of the β chains (see Table 4). The other His residue are buried and are presumed in the NMR study to have their pK_a values outside the pH range [4−9] accessible to the NMR measurements. The pK_a^{eff} values of all His residues are calculated, including those not observed in the NMR experiments; almost all of latter values are found to have pK_a^{eff} values outside the accessible pH range.

Deoxy and Oxy Structures of HbA. We present a number of the characteristics of relatively high resolution deoxy and oxy X-ray structures for HbA available in the literature; the use of the term oxy is a shorthand for liganded, whether CO, O_2, or NO.[45−48] In Table 1, we list the structures, their nominal resolution, and the original reference; for deoxy HbA, we include only structures with a resolution 2 Å or better, while for oxy HbA, we include lower resolution structures, some of which have been suggested to be ″the″ oxy HbA structure in solution.[19] The structures were crystallized under different conditions (e.g., pH, salt concentration, temperature, as described in the references in Table 1). The RMSD values between pairs of

dx.doi.org/10.1021/bi401126z | Biochemistry 2013, 52, 8539−8555

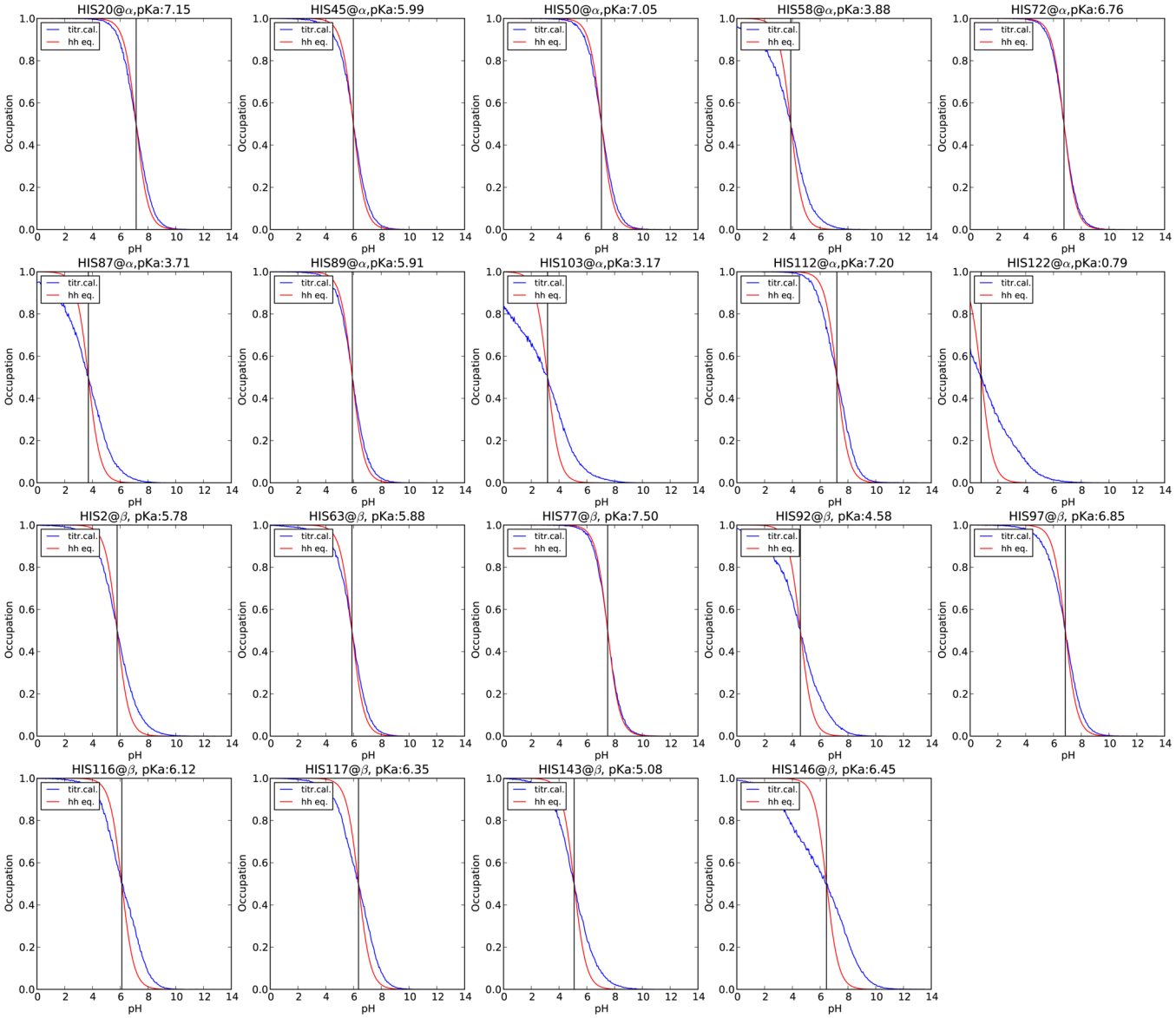

Figure 4. Average protonation curves of His^+ state of all His residues for 2DN3(Oxy) from titration calculations and Henderson−Hasselbalch equation. The black line corresponds to the pK_a^{eff} value.

crystal structures are listed in Table 2. The heavy atom RMSD between X-ray structures for deoxy HbA range from 0.55 Å to 0.95 Å, while those for the oxy X-ray structures vary over a significantly larger range (from 1.39 Å to 3.03 Å). For comparison, we note that the RMSD between deoxy and oxy HbA structures, also shown in the table, is in the range of 2.65−4.20 Å, similar to the range of variation of the oxy structures among themselves.

As stated in Computational Details, we generated three additional structures from the X-ray structures. We focus on the minimized WHATIF structures (Table 3); data for the other structures are given in Supporting Information. In the highest resolution structure, 2DN2 and 2DN3, WHATIF introduced no changes in 2DN2 and three changes in 2DN3. For comparison, in the lower resolution structure, 1HHO(R), there are eight changes. The specific changes for all structures are given in Table S10 in the Supporting Information. Overall, the distribution of RMSD values between structures of the four sets of structures are very similar, with the RMSD's always much smaller for the deoxy than the oxy structures. The deviations of the minimized WHATIF structures from the crystal structures of both deoxy and oxy HbA are similar and small (in the range of 0.6 to 0.8 Å) and the difference between the minimized and unminimized WHATIF structures are of the same order. As described in Caves et al.,[49] the structures tend to move on a "hypersurface" under small perturbations, remaining approximately equidistant from each other. However, although the structural differences are not large, they can result in significant changes in the calculated pK_a^{eff} values, so that a comparison of the results from a number of them is of interest.

Deoxy HbA pK_a^{eff} Calculations. The calculated pK_a values, i.e., pK_a^{eff}, and their deviations from experiment for the measured His residues (in parentheses) are listed in Table 4 for the minimized WHATIF structures, and Tables S2 to S4 for the other structures. Although the effect of minimization is not large, it does lead to improved agreement with experiment on average. This is true for minimization of the crystal structures and minimization of the WHATIF optimized structures.

For the minimized WHATIF structures, all predicted changes of the pK_a^{eff}'s from the solution value are in the right

dx.doi.org/10.1021/bi401126z | Biochemistry 2013, 52, 8539−8555

direction. 2DN2 (and 2DN3 for oxy Hb) are used for most of the analysis because they are the highest resolution structures and were determined under the same conditions; the results obtained with them are listed in bold in the tables. The magnitude of the average prediction error is around 0.5 pK_a units (0.7 kcal/mol) and the maximum error is less than 1 pK_a unit (1.4 kcal/mol), with the exception of His117@β1 of 2DN2. Interestingly, the β2 chain has a smaller error for His117; the difference is due to the fact that the whole protein does not exactly have C_2 symmetry and the WHATIF program predicts a different hydrogen bonding network around His117 in the two β chains. As we shall see for oxy HbA, the variations of the calculated pK_a^{eff} values with the structure used tend to be significantly larger, in accord with the fact that the structures differ more.

Although the available NMR data for HbA do not distinguish between N^{δ} and N^{ε} of His in the single protonated (neutral) form, we show in Figure 1 the calculated protonation states of the His sites of 2DN2 as a function of pH. The His^+ occupation corresponds to the titration curve of the residue and the 50% protonated state corresponds to the value of pK_a^{eff}. Most of the calculated total titration curves, the blue line in Figure 1 corresponding to the His^+ curve, have the simple form expected from the Henderson−Hasselbalch equation (see Figure 2). However, there are some that differ significantly, for example His103 and His107. Also, as shown in Figure 2 for His β146, the deviation is small in 2DN2 but large in 2DN3 (Figure 4). In the neutral form, some His (e.g., β146) have mainly N^{ε} protonated, others (e.g., β143) have N^{δ} and N^{ε} approximately equally protonated, and still others (e.g., α50) have mainly N^{δ} protonated.

As mentioned earlier, a number of the His pK_a's were not accessible to NMR in the measurable pH range[4−9] in both deoxy and oxy HbA. They are α58, α87, α103, α122, β63, and β92. All of them are predicted to have a low pK_a^{eff} (see Table 4 and Table 5) though not all are predicted to be below 4 (α58, β63). All of the residues that are not observed are essentially buried with exposed surface areas less than 10%, except for β63 in the oxy structure; there are also some residues with low exposed surface areas, which are in the measurable range (e.g., β97 and β116) in both the deoxy and oxy structures. Since buried residues are expected to be more sensitive to the dielectric constant due to the Born contribution, we have repeated the calculation for a dielectric constant of 4 (see Table S8 in SI).

Oxy HbA pK_a^{eff} Calculations. The calculated pK_a values, i.e., pK_a^{eff}, and their deviations from experiment (in parentheses) are listed in Table 5 for the minimized WHATIF structures and in Tables S5 to S7 for the other structures. A striking result is that for both His β143 and His β146, only the 2DN3 structure yields close agreement with experiment and that all other structures have large errors in His β146 and several also have large errors in His β143; these two residues contribute most to the Bohr alkaline and acid effects, respectively. As shown in Table 3, the oxy structures differ significantly more from each other than do the deoxy structures. Not unexpectedly, this is reflected in the pK_a^{eff} values. For the residues other than *His*β146 and *His*β143, all the structures have errors less than 1.5 pK_a units (2 kcal/mol). The average error of 2DN3 is 0.3 pK_a units (0.4 kcal/mol) and the maximum error is 0.9 pK_a units (1.3 kcal/mol). Figure 3 shows the titration curves for all the His residues calculated with 2DN3. As for deoxy HbA, most curves are close to single titration behavior (see Figure 4). However, His β146, in particular, is an exception. In most cases,

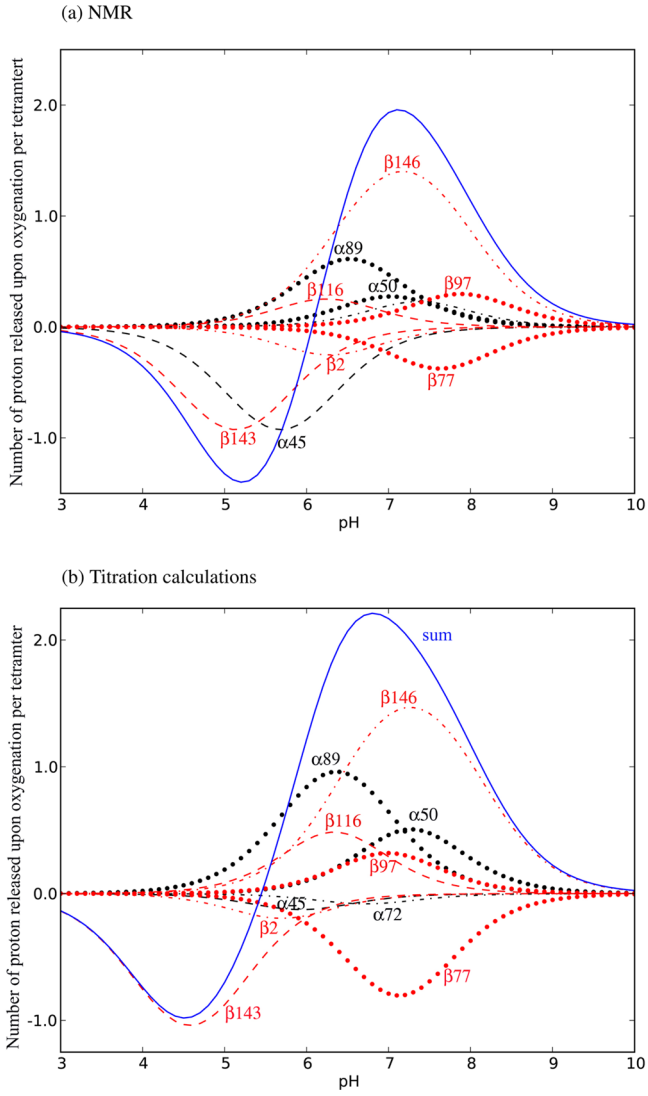

Figure 5. Contributions of all His residues to the Bohr effect except α20, α112, and β117 whose contributions are negligible.

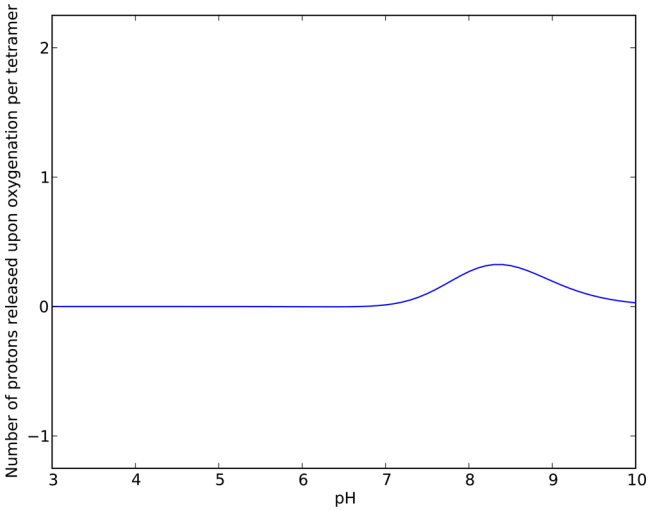

Figure 6. Proton release curve of HbA upon oxygenation for Val1@α.

for neutral His, the same position (N^{δ} or N^{ε}) tends to be favored in oxy HbA as in deoxy HbA for a given residue and to the same degree. However, there are cases (e.g., His β77)

dx.doi.org/10.1021/bi401126z | *Biochemistry* 2013, 52, 8539−8555

Table 6. Born Energy, Background Interaction Energy, and pK_a^{intr} of His143 and His146 in the Minimized WHATIF 2DN2 and 2DN3 Structures[a]

(a) 2DN2

		His^+		N^ε		N^δ		
site	pK_a^{stnd}	Born	background	Born	background	Born	background	pK_a^{intr}
His143	6.38	0.521	−0.316	0.116	0.034	0.130	−0.113	6.25
His146	6.38	0.578	−0.422	0.138	0.025	0.153	0.068	6.44

(b) 2DN3

		His^+		N^ε		N^δ		
site	pK_a^{stnd}	Born	background	Born	background	Born	background	pK_a^{intr}
His143	6.38	0.562	−0.437	0.136	0.025	0.140	−0.111	6.23
His146	6.38	0.855	−0.869	0.208	0.305	0.191	−0.004	6.23

[a]All values are given in pK units.

where the N^ε/N^δ ratio is different in the two structures, particularly (and not surprisingly) for residues with small shifts.

Most residues are shifted less in the oxy structure from pK_a^{stnd}. Probably as a consequence of the smaller pK_a shift, the errors of the oxy HbA pK_a^{eff} values tend to be smaller than those of the deoxy values. Both His β143 and His β146 are shifted less from the solution value in oxy than in deoxy HbA; His β143 is shifted in the same direction (to a lower value) in both deoxy and oxy HbA, while His β146 is shifted upward by a large amount in deoxy HbA, and it is shifted downward by a small amount in oxy HbA.

Bohr Effect. His residues make the major contributions to both the alkaline and the acid Bohr effects, as shown by the site specific NMR measurements of Ho and co-workers.[19] Figure 5 shows Bohr effect obtained from the NMR measurement (Figure 5a) and from the calculated pK_a^{eff} values (Figure 5b) in terms of the total proton release upon oxygenation by the HbA tetramer and the contribution of each His to the total. The number of released protons from each His residue, ΔH_i, is calculated based on the standard relation

$$\Delta H_i = 2\left(\frac{K_i^{oxy}}{[H^+] + K_i^{oxy}} - \frac{K_i^{deoxy}}{[H^+] + K_i^{deoxy}}\right) \quad (10)$$

where the K's are proton dissociation constants and $[H^+]$ is the hydrogen ion concentration. Although the curves in Figure 5a and Figure 5b are not identical, they are quite similar for both the alkaline Bohr effect (normally referred to as "the" Bohr effect) and the acid Bohr effect. The largest error occurs for the contribution of α45 to the acid Bohr effect due to the fact that the 2DN3 result is nearly exact (error of 0.02), while the downward shift in 2DN2 (error of 0.63) is too small. Based on the His residues, the maximum alkaline Bohr effect (2.0 protons released) is observed experimentally at pH 7.4 (the calculated values are 2.12 proton released at pH 7.1) and the maximum acid Bohr effect (1.0 protons absorbed) occurs at pH 5.1 (the calculated values are 0.98 protons absorbed at pH 4.5). The corresponding values from oxygenation measurements for the maxima are at pH 7.1 and 5.2, respectively, with 1.96 protons released and 1.40 absorbed.[19] Since the Bohr effect depends on the ligand and the presence of other effectors, we remind the reader that the experimental and the calculated results reported here are for stripped deoxy HbA and CO HbA. The agreement is satisfactory and confirms that His β146 makes the largest contribution to the alkaline Bohr effect, while His β143 makes the dominant contribution to the acid Bohr effect; His α45 appears experimentally almost equally important as His β143 for the latter, but it has the largest measurement uncertainty.

Table 7. Interaction Free Energy for His143 and His146 for deoxy 2DN2 (WHATIF Minimized) Structures of Residues out to 15 Å[a]

(a) Interaction Free Energy E_{ij} between His143 and Other Residues

Res_i	Prot. State	Res_j	Prot. State	Distance [Å]	E_{ij} [kcal/mol]
His143@β1	charged	Lys82@β1	charged	5.18	0.31
His143@β1	charged	Lys144@β1	charged	5.62	0.32
His143@β1	charged	Tyr145@β1	neutral	9.47	−0.17
His143@β1	charged	Glu90@β1	charged	9.70	−0.14
His143@β1	charged	His146@β1	charged	10.95	0.14
His143@β1	charged	His2@β2	charged	11.48	0.15
His143@β1	charged	Nter@β1	charged	11.97	0.15
His143@β1	charged	Cter@β1	charged	12.39	−0.11
His143@β1	charged	Lys132@β2	charged	12.52	0.16
His143@β1	charged	Nter@β2	charged	12.75	0.15
His143@β1	charged	rg104@β1	charged	13.17	0.16
His143@β1	charged	His92@β1	charged	13.27	0.12
His143@β1	charged	Lys82@β2	charged	13.93	0.15

(b) Interaction Free Energy E_{ij} between His146 and Other Residues

Res_i	Prot. State	Res_j	Prot. State	Distance [Å]	E_{ij} [kcal/mol]
His146@β1	charged	Cter@β1	charged	3.22	−0.58
His146@β1	epsilon	Cter@β1	charged	3.22	0.20
His146@β1	charged	Asp94@β1	neutral	5.84	−0.11
His146@β1	charged	Asp94@β1	charged	5.84	−0.95
His146@β1	epsilon	Asp94@β1	charged	5.84	−0.23
His146@β1	charged	Tyr145@β1	eutral	16	−0.22
His146@β1	charged	Lys40@α2	charged	7.32	0.34
His146@β1	charged	Glu90@β1	charged	8.02	−0.20
His146@β1	charged	Lys144@β1	charged	8.43	0.17
His146@β1	charged	His97@β1	charged	10.87	0.17
His146@β1	charged	Lys95@β1	charged	10.94	0.14
His146@β1	charged	His143@β1	charged	10.95	0.14
His146@β1	charged	Lys132@β2	charged	11.82	0.17
His146@β1	charged	His92@β1	charged	12.99	0.12
His146@β1	charged	Glu7@β2	charged	13.49	−0.14

[a]The distance is measured between geometric centers of the side chain atoms of the residue pairs.

Contributions to the Bohr Effect from Residues Other than Histidines. To determine whether residues other than His contribute to the Bohr effect, we have done corresponding calculations of pK_a^{eff} in deoxy and oxy HbA for all titratable

dx.doi.org/10.1021/bi401126z | Biochemistry 2013, 52, 8539−8555

Table 8. Interaction Free Energy for His143 and His146 of Oxy 2DN3 (WHATIF Minimized) Structures of Residues out to 15 Å[a]

(a) Interaction Energy E_{ij} between His143 and Other Residues

Res_i	Prot. State	Res_j	Prot. State	Distance [Å]	E_{ij} [kcal/mol]
His143@β1	charged	Lys82@β1	charged	5.41	0.28
His143@β1	charged	Lys144@β1	charged	5.96	0.30
His143@β1	charged	Cter@β1	charged	6.52	−0.36
His143@β1	charged	His146@β1	charged	6.68	0.33
His143@β1	charged	Glu90@β1	charged	8.36	−0.19
His143@β1	charged	Nter@β2	charged	8.84	0.26
His143@β1	charged	His2@β2	charged	9.62	0.19
His143@β1	charged	Tyr145@β1	neutral	10.20	−0.14
His143@β1	charged	Asp94@β1	charged	10.38	−0.20
His143@β1	charged	His146@β2	charged	11.20	0.19
His143@β1	charged	Cter@β2	charged	12.34	−0.17
His143@β1	charged	His92@β1	charged	12.69	0.13
His143@β1	charged	Nter@β1	charged	12.70	0.16
His143@β1	charged	His143@β2	charged	13.02	0.15

(b) Interaction Energy E_{ij} between His146 and Other Residues

Res_i	Prot. State	Res_j	Prot. State	Distance [Å]	E_{ij} [kcal/mol]
His146@β1	charged	Cter@β1	neutral	4.15	0.12
His146@β1	charged	Cter@β1	charged	4.15	−0.54
His146@β1	charged	His143@β1	charged	6.68	0.33

(b) Interaction Energy E_{ij} between His146 and Other Residues

Res_i	Prot. State	Res_j	Prot. State	Distance [Å]	E_{ij} [kcal/mol]
His146@β1	charged	Nter@β2	charged	7.16	0.31
His146@β1	charged	Tyr145@β1	neutral	7.33	−0.29
His146@β1	charged	His146@β2	charged	7.50	0.51
His146@β1	charged	His2@β2	charged	9.35	0.21
His146@β1	charged	Lys144@β1	charged	9.60	0.12
His146@β1	charged	Cter@β2	charged	10.70	−0.24
His146@β1	charged	His143@β2	charged	11.20	0.19
His146@β1	charged	Lys82@β1	charged	11.24	0.10
His146@β1	charged	Lys132@β2	charged	11.73	0.14
His146@β1	charged	Arg104@β2	charged	11.95	0.31
His146@β1	charged	Asp94@β1	charged	12.07	−0.16
His146@β1	charged	Nter@β1	charged	12.60	0.20
His146@β1	charged	Asp99@β1	charged	12.83	−0.32
His146@β1	charged	His92@β1	charged	13.49	0.16
His146@β1	charged	Glu101@β1	charged	13.73	−0.30
His146@β1	charged	Tyr145@β2	neutral	13.85	−0.17
His146@β1	charged	Arg104@β1	charged	14.06	0.26
His146@β1	charged	Glu101@β2	charged	14.39	−0.30
His146@β1	charged	His97@β1	charged	15.00	0.11

[a]The distance is measured between geometric centers of two side chain atoms of the residue pairs.

residues. It turns out that the only other residues that can contribute are the N terminal group of Val α1 and Val β1. All other residues titrate outside the pH range of interest for the Bohr effect.

For Val α1 the calculated values of the pK_a^{eff} are 8.60 and 7.80 in deoxy and oxy HbA, yielding the Bohr effect curve shown in Figure 6. The number of protons released from the two chains at pH 8.4 is 0.32, corresponding to 16% of the Bohr effect at that pH. For Val β1, we find that the pK_a^{eff} shift is in the direction favoring oxy Hb, which would lead to an inverse Bohr effect. However, we note that the presence of Cl^- in the neighborhood of the BPG binding site would be expected to stabilize the protonated form in deoxy HbA and could neutralize (or reverse) the effect of this group; Cl^- ions were not included in the model.

Mutant and modification studies[50,51] have suggested that other residues contribute to the Bohr effect. One example is Glu β43, where amidation of the carboxyl group alters the Bohr effect. The calculated pK_a^{eff}'s of Glu β43 are 3.03 and 3.55 in deoxy and oxy HbA respectively; i.e., they are in a range far outside that of the alkaline Bohr effect (and the change is in the wrong direction). This suggests that it is not the carboxyl group, *per se*, that is involved, but rather the amidation experiments measure an effect on the titration of another Bohr group. It could be a structural perturbation, such as that found previously in the analysis of the effect of a mutation of Asp in tRNA.[52]

Analysis of Origin of the pK_a^{eff} shifts. Providing insights into the origin of the pK_a shifts from pK_a^{stnd} to pK_a^{eff} is an important objective of this paper, in particular because it is difficult to make an experimental determination of the contributions by structural or mutation studies. As described in the section Methodology and Computational Details, we use two approaches to estimate the contributions from all other protein residues to the pK_a shift of a given residue, relative to pK_a^{stnd}, the measured solution value. The first method calculates the values of the interaction free energy between the residue of interest and other residues (eq 4a), in addition to the background term (eq 4b) and the Born term (eq 4c). The analysis is focused primarily on the important residues His β146 and His β143. The contributions to the value of pK_a^{intr} (see eq 9), relative to pK_a^{stnd}, are listed in Table 6. Although the Born energy and background energy contributions to the pK_a shift are significant, their sum is not. Consequently, the pK_a^{intr} values of both His β143 and His β146 in 2DN2 and 2DN3 deviate little from the pK_a^{stnd} values.Table 7 and Table 8, respectively, show the interaction energy E_{ij} and pK_a shift contribution of various protein residues to the residue of interest for 2DN2 and 2DN3. We include all residues that are significant within 15 Å. For His β146 of 2DN2, the C terminal carboxylic group, which makes a salt bridge to Lys 40 α_2, and the salt bridge with Asp94 have the largest stabilizing interaction free energy. Interestingly, the C terminal carboxylic group has, in addition, a destabilizing interaction with N^{ε}, while Asp94 has a stabilizing interaction with N^{ε}. A number of other residues are significant; see Figure 7.

For Hisβ146 in 2DN3 as in 2DN2, the C terminal carboxy group has a similar stabilizing interaction free energy (−0.54 kcal/mol), but Asp94 β_1 is 17 Å from His β146, so that it makes a much smaller contribution. Interestingly, there are residues up to a distance of 21 Å which make contributions of greater than 0.1 kcal/mol, both positive and negative in oxy HbA. This appears to arise from the fact that in oxy HbA, His β146 is 90% buried; in deoxy, His β146 is essentially on the surface (35% buried).

For His β143 in 2DN2, Lys β82 and Lys β144 make the dominant destabilizing interaction free energy contribution (0.31 and 0.32 kcal/mol, respectively); in 2DN3, these two groups make similar destabilizing contributions (0.25 and 0.30 kcal/mol, respectively). Figure 7 shows some of the important residues. The actual calculated pK_a^{eff} downward shift on oxygeneration is somewhat overestimated (see Table 5).

The perturbation results obtained for His β146 and His β143 in 2DN2 and 2DN3 are shown in Figure 8. Not surprisingly, the residues that are found to produce significant interaction

dx.doi.org/10.1021/bi401126z | Biochemistry 2013, 52, 8539−8555

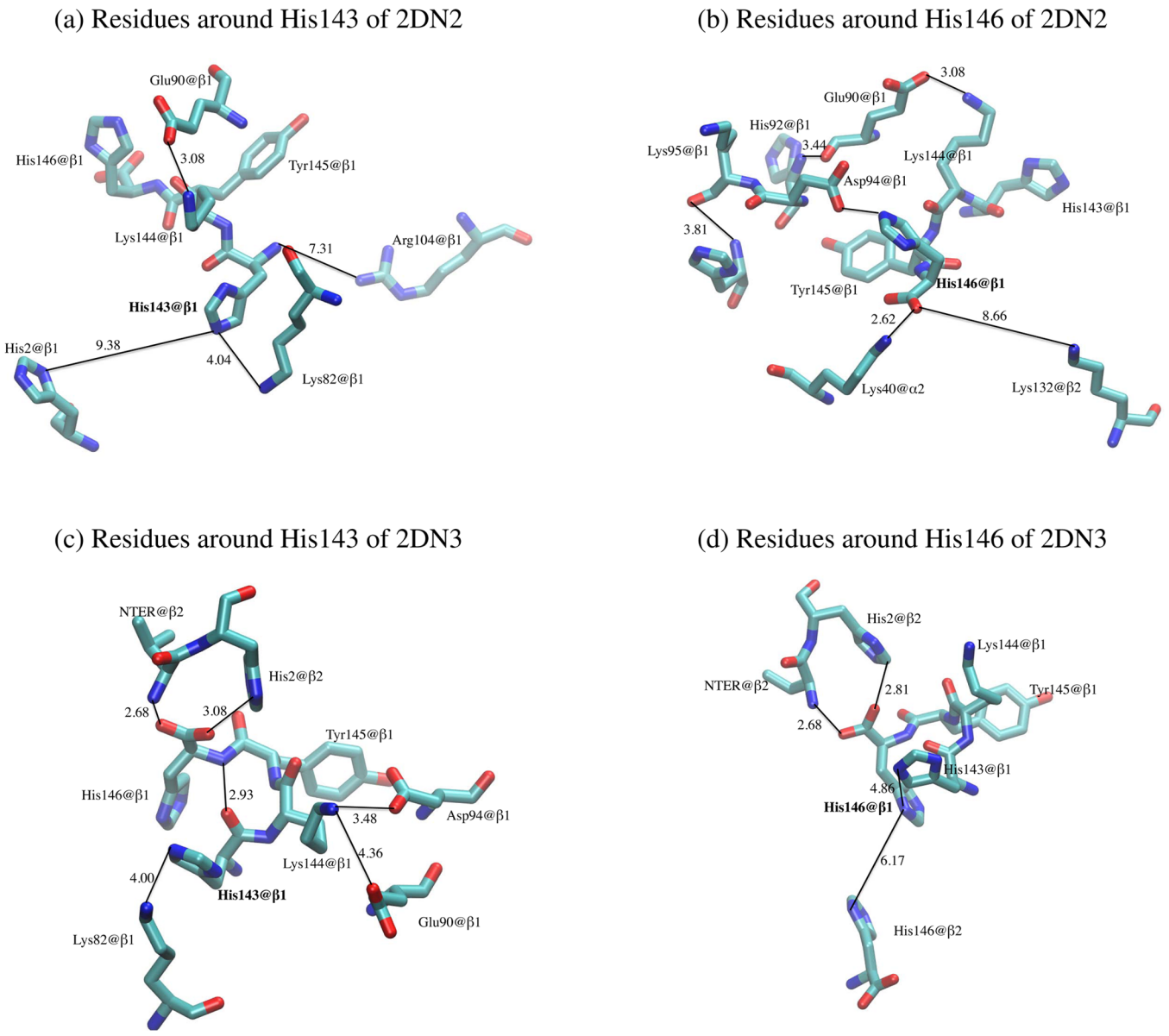

Figure 7. Important residues for His143 and His146 in 2DN2 and 2DN3. For clarity, some residues listed in Table 7 and Table 8 that are more distant are not shown.

free energies are essentially the same as those that contribute to the perturbation analysis. However, the perturbation analysis makes possible an estimate of the contributions of the various residues to the pK_a^{eff} shift. For both His β146 and His β143 in 2DN2, the perturbation result is in satisfactory agreement with the full calculation in Table 5. For 2DN3, the perturbation analysis works for Hisβ143 but breaks down for Hisβ146, in accord with the fact that double mutant cycles show significant coupling. This is likely to be due to the fact, already mentioned, that Hisβ146 is significantly buried in 2DN3 structure.

CONCLUDING DISCUSSION

Although the Bohr effect in hemoglobin was discovered more than one hundred years ago, a complete understanding of its origins is not available. It is now known that there is both an alkaline and an acid Bohr effect. The former corresponds to the release of protons on oxygenation at alkaline pH and the latter corresponds to the uptake of protons on oxygenation at acid pH. Based on the structures of unliganded (deoxy) and liganded (met)HbA, Perutz proposed that the alkaline Bohr effect was due to two pairs of salt bridges (see Figure 9), present in deoxy hemoglobin and absent in oxy hemoglobin. Mutant studies supported the Perutz model,[8] but they also suggested that other residues could be involved. It is only relatively recently that NMR studies of deoxy and carbonmonoxy HbA demonstrated that His residues play the dominant role in both the alkaline and acid Bohr effect with His β146 being most important for the former and His β143 for the latter. In this paper we calculate the pK_a shifts in deoxy and oxy HbA, relative to the solution values of model compounds, to obtain pK_a^{eff}, the pK_a value in the protein, and use the results to determine the origin of the shift at the molecular level. For this purpose, the electrostatic free energy of the system as a function of the protonation states of the titratable residues is determined for a set of pH values by solving the linearized finite-difference Poisson−Boltzmann equation. The free energy consists of the desolvation free energy of the titratable residues, the electrostatic free energies

dx.doi.org/10.1021/bi401126z | Biochemistry 2013, 52, 8539−8555

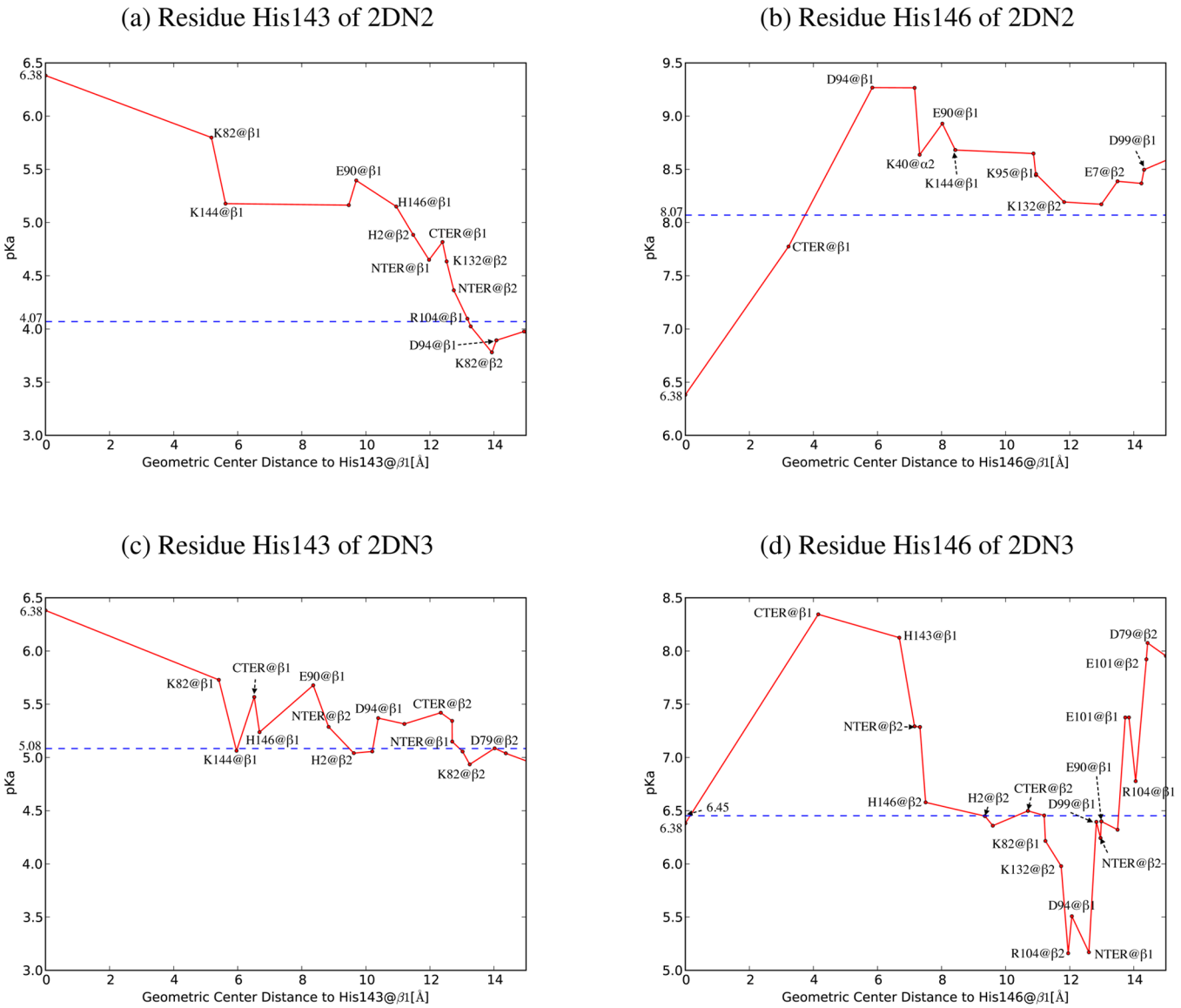

Figure 8. Perturbational analysis of residues contributing to the pK_a^{eff} in His143 and His146. The points are the cumulative sum of those within the current distance; the standard pK_a value in aqueous solution is indicated on the point where the red line intersects with the *Y* axis and the calculated residue pK_a value in protein, i.e., pK_a^{eff}, is indicated by the dash line. "NTER" and "CTER" refer to the N terminus and C terminus, respectively.

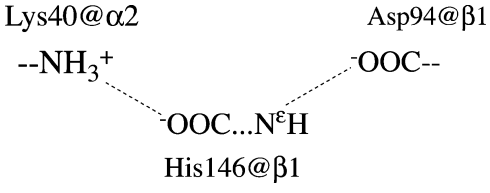

Figure 9. Perutz salt bridges in Deoxy HbA involving His146 at *β*1. Redrawn from reference 11.

of interaction between titratable residues and background atoms (fixed charged residues and polar groups) and between titratable residues in the given protonation states. Because of the large number of titratable residues in HbA, Monte Carlo sampling is used to determine their average proton states and their pK_a^{eff}. With the highest resolution minimized WHATIF structures for deoxy and carbonmonoxy HbA, there is good agreement between the calculated pK_a^{eff} and the experimental pK_a's for the His residues that have been measured. These include six out of a total of ten His in each *α* chain and seven out of a total of nine His in each *β* chain. The calculations show that the His residues that are not observed have their pK_a^{eff} values shifted to low pH beyond the observable range (pH 4 to 9) due to the large Born desolvation contribution resulting from their being mainly buried, in contrast to most of the observable His residues, which are exposed to the solvent.

The only residues, other than the His, that are calculated to contribute significantly to the alkaline Bohr effect are the amino terminal groups of Val1 in the *α* chains and *β* chains. Other residues (e.g., Glu *β*40 and Lys82) that have been suggested as alkaline Bohr groups from mutation experiments cannot contribute directly, according to the calculations. Rather, they must produce their effect by perturbing the protein so as to change the His contributions.

Given the agreement between the experimental and the calculated pK_a^{eff} values, we use the latter to obtain insights concerning the origin of the alkaline and acid Bohr effects beyond those available from experiment. Since the pK_a shifts, relative to

dx.doi.org/10.1021/bi401126z | *Biochemistry* 2013, 52, 8539−8555

the model compound values, in deoxy HbA are generally significantly larger than in carbonmonoxy HbA, we focus primarily on the former. Using the calculated free energy of interaction and a complementary perturbation approach, we show that for β146, which makes the dominant contribution to the alkaline Bohr effect, the Perutz salt bridge between Asp β94 and the N^{ε} of the His side chain is most important. For β143, which makes the dominant contribution to the acid Bohr effect, Lys 82β1 and Lys 144 β1 are dominant. However, in both cases, other interactions that extend to 15 Å from β146 and β143 make non-negligible contributions.

The sensitivity of the calculated results to the details of the structure used is of particular interest for the oxy structures, which vary over a range of 4 Å in their RMSD and have significant difference in the calculated pK_a^{eff} values. The results suggest that the solution structure is close to the carbonmonoxy structure (2DN3), rather than to R2 or other structures that have been determined by X-ray diffraction under various conditions. However, we cannot exclude the possibility that some mixture of structures that agree as well as 2DN3 with the measured pK_a values represent the oxy HbA ensemble present in solution.

The present analysis provides support of the Perutz model for the Bohr effect as a zero-order description. However, His residues other than His β146 make significant contributions and the pK_a^{eff} shift of Hisβ146 in deoxy HbA is due not only to the Perutz salt bridges, but also to other interactions.

APPENDIX

In this appendix, we give a summary of the programs and scripts used for the pK_a calculations. They were developed by one of the authors (M. Schaefer).

Main Program

The calculations in this work were performed by a collection of computer programs, where the workflow leading from the structure to the titration curves is controlled by a single script written in the UNIX csh language. In this script, termed "pk_run", the calculation is divided into the steps "initialization", "electrostatics calculation", and "titration curve calculation".

Initialization

During initialization, the input structure in CHARMM crd format and a parameter file specifying titratable sites are used to produce input for the subsequent calculations, in particular, the list of the titrating sites that are present in the system and separate coordinate files in pdb format for the model compounds. Titrating sites in the input structure are identified by residue and atom names that match an entry in the parameter file. The residue names for titrating N and C-terminal atoms are given as NTER and CTER in the parameter file and must be changed accordingly in the input structure file if they are to be included in the titration calculation. Two copies of the input structure in crd format are required, one with atom radii and the other with partial charges in the 10th data column, which is equivalent to the "pqr" format that is frequently used as input to Poisson-Boltzmann calculations.[53] The partial charges of background atoms are employed as given in the charge-crd file, whereas the partial charges of titrating sites are taken from the parameter file because they vary according to the protonation state. For every titrating site, the residue containing the site is written out as its model compound, i.e., without adding terminal blocking groups.

Electrostatics Calculation

As described in Methods, to compute the electrostatic energy of the system or a model compound in a given protonation state, $E(s)$, it is necessary to determine the electrostatic interaction energy between every pair of atom groups (including the background atoms) with atom partial charges according to their protonation state, $E_{ij}(s_i, s_j)$. This is done by performing Poisson-Boltzmann calculations for every site and protonation state in the protein, and in the model compounds. One additional calculation for the system and each model compound is concerned with the non-titrating background atoms. At the beginning of each Poisson-Boltzmann calculation, only the atoms of site i are assigned partial charges according to the protonation state s_i; all other atoms are uncharged. The solution of the Poisson-Boltzmann equation is then used to determine the electrostatic potential ϕ_i of site i throughout the system, from which the interaction with site j in protonation state s_j is computed by the sum $E_{ij}(s_i,s_j) = \sum_k q_k(s_j)\phi_i(s_i)$, where the sum is over all atoms k of site j. The Poisson-Boltzmann program UHBD is implemented with the script pk_run to perform this task, making use of the UHBD commands for assigning charges to individual atoms, printing out the electrostatic potential, and computing the solvation free energy of a set of charges corresponding to the diagonal terms $E_{ii}(s_i,s_i)$. Other programs, e.g., the multigrid Poisson-Boltzmann program APBS[53] or generalized Born electrostatic methods[54,55] offer similar functionality and could be equivalently employed. The output of the electrostatic calculations is stored in two files, one for the system and all pairs of sites i, j, the other with data on all model compounds. Since the Poisson-Boltzmann calculations for all sites and model compounds are independent, the main script offers parallel processing for the UHBD calculations.

Titration Calculation

Three programs are available for computing titration curves and pKa's of all sites according to eq 5: "titrex" for a full enumeration of all protonation states of the system, applicable to approximately 30 titrating sites; a parallelized version, "titrex_p" which extends the range of applicability, e.g., by a factor of 10 for 1000 compute nodes; and "titrmc", which computes titration curves by Monte Carlo sampling. The input of the titration programs is the list of all sites with the standard pK_a values and the output from the electrostatic energy calculations on the system and model compounds. The output are the probabilities of all sites and protonation states over a user-defined pH-range. The titration programs are not restricted to two protonation states; in particular, they can treat the case of His residues with 3 possible states. Similar to the Beroza method,[44] the Monte Carlo titration program uses exchange of H+ with the solvent and between "coupled" sites as Monte Carlo steps. However, it differs from that of Beroza by the fact that it can handle multiple (>2) protonation states. Finally, a separate program reads the titration curve data and derives effective pK_a values of all site, giving an upper or lower bound if they are outside the computed pH-range.

The program is available from its author (M. Schaefer, michael.schaefer@novartis.com).

ASSOCIATED CONTENT

Supporting Information

The atomic charges of all titratable residues are given in Table S1. The His experimental (NMR) and calculated pK_a values of deoxy HbA WHATIF structure, minimized crystal structure, and crystal

structure for PDB code 2DN2, 4HHB, 1BZ0, 1RQ3, 1XXT, and 1KD2 are given in Table S2, S3, and S4, respectively. The His experimental (NMR) and calculated pK_a values of oxy HbA WHATIF structure, minimized crystal structure, and crystal structure for PDB code 2DN3, 1HHO, 1BBB, 1MKO, and 1YZI are given in Table S5, S6, and S7, respectively. Table S8 lists the His experimental (NMR) pK_a value and calculated pK_a values using different dielectric constants of the solvent, and the surface exposure percentage of each His residue for both deoxy 2DN2 and oxy 2DN3 structures. The calculated His pK_a value differences between two dimers of HbA for both deoxy 2DN2 and oxy 2DN3 are shown in Table S9. This material is available free of change via the Internet at http://pubs.acs.org.

AUTHOR INFORMATION

Corresponding Author

*E-mail: marci@tammy.harvard.edu. Phone: 1-617-495-4018. Fax: 1-617-496-3204.

Funding

NIH grant No. R01-GM030804.

Notes

The authors declare no competing financial interest.

ACKNOWLEDGMENTS

We gratefully acknowledge helpful discussions with Dr. Victor Ovchinnikov and Dr. Robert Petrella. The computations were run on the Odyssey cluster at Harvard University and on computers of the National Energy Research Scientific Computing Center (NERSC), which is supported by the Office of Science of the U.S. Department of Energy (DOE) under Contract No. DE-AC02-05CH11231.

REFERENCES

(1) Antonini, E., and Brunori, M. (1970) Hemoglobin. *Annu. Rev. Biochem. 39*, 977−1042.

(2) Bohr, C. (1903) Theoretische Behandlung der quantitativen Verhältnisse der Kohlensäurebindung des Hämoglobins. *Zentralblatt Für Physiologie XVII*, 713−716.

(3) Bohr, C., Hasselbalch, K., and Krogh, A. (1904) About a new biological relation of high importance that the blood carbonic acid tension exercises on its oxygen binding. *Skandinavisches Archiv Fur Physiologie 16*, 404−412.

(4) Edsall, J. T. (1980) Hemoglobin and the origins of the concept of allosterism. *Federation Proceedings 39*, 226−235.

(5) Christiansen, J., Douglas, C., and Haldane, J. (1914) The absorption and discussion of carbon dioxide by human blood. *Journal of Physiology-London 48*, 244−271.

(6) Brunori, M. (2012) The Bohr effect before Perutz. *Biochem. Mol. Biol. Educ. 40*, 297−299.

(7) Rossifanelli, A., Antonini, E., and Caputo, A. (1964) Hemoglobin and Myoglobin. *Adv. Protein Chem. 19*, 73−222.

(8) Kilmartin, J., and Rossi-Bernardi, L. (1973) Interaction of hemoglobin with hydrogen ions, carbon dioxide, and organic phosphates. *Physiol. Rev. 53*, 836−890.

(9) Riggs, A. F. (1988) The Bohr effect. *Annu. Rev. Physiol. 50*, 181−204.

(10) Perutz, M. F. (1970) Stereochemistry of cooperative effects in hemoglobin. *Nature 228*, 726−734.

(11) Perutz, M. F., and Ten Eyck, L. F. (1970) Stereochemistry of cooperative effects in hemoglobin. *Cold Spring Harbor Symp. Quantum Biol. 36*, 295−310.

(12) Szabo, A., and Karplus, M. (1972) Mathematical model for structure-function relations in hemoglobin. *J. Mol. Biol. 72*, 163−197.

(13) Szabo, A., and Karplus, M. (1972) Mathematical model for structure-function relationships in hemoglobin. *Biochem. Biophys. Res. Commun. 46*, 855−860.

(14) Monod, J., Wyman, J., and Changeux, J. P. (1965) On the nature of allosteric transitions: a plausible model. *J. Mol. Biol. 12*, 88−118.

(15) Roughton, F. J. W., and Lyster, R. L. J. (1965) *Hvalradets Skrifter 48*, 185−198.

(16) Lee, A. W. M., and Karplus, M. (1983) Structure-specific model of hemoglobin cooperativity. *Proc. Natl. Acad. Sci. U.S.A. 80*, 7055−7059.

(17) Henry, E. R., Bettati, S., Hofrichter, J., and Eaton, W. A. (2002) A tertiary two-state allosteric model for hemoglobin. *Biophys. Chem. 98*.

(18) Eaton, W. A., Henry, E., Hofrichter, J., Bettati, S., Viappiani, C., and Mozzarelli, A. (2007) Evolution of allosteric models for hemoglobin. *IUBMB Life 59*, 586−599.

(19) Ho, C., and Yuan, Y. *Haemoglobin: Cooperativity in Protein-Ligand Interactions*; Encyclopedia of Life Sciences ed.; John Wiley Sons, Ltd, 2010; pp 1−6.

(20) Fang, T.-Y., Zou, M., Simplaceanu, V., Ho, N. T., and Ho, C. (1999) Assessment of roles of surface histidyl residues in the molecular basis of the bohr effect and of beta 143 histidine in the binding of 2,3-bisphosphoglycerate in human normal adult hemoglobin. *Biochemistry 38*, 13423−13432.

(21) Bashford, D., and Karplus, M. (1990) pKas of ionizable groups in proteins - atomic detail from a continuum electrostatic model. *Biochemistry 29*, 10219−10225.

(22) Lim, C., Bashford, D., and Karplus, M. (1991) Absolute pKa calculations with continuum dielectric methods. *J. Phys. Chem. 95*, 5610−5620.

(23) Bashford, D., Case, D. A., Dalvit, C., Tennant, L., and Wright, P. E. (1993) Electrostatic calculations of side-chain pKa values in myoglobin and comparison with NMR data for histidines. *Biochemistry 32*, 8045−8056.

(24) Antosiewicz, J., Mccammon, J., and Gilson, M. K. (1994) Prediction of pH-dependent properties of proteins. *J. Mol. Biol. 238*, 415−436.

(25) Yang, A. S., Gunner, M. R., Sampogna, R., Sharp, K., and Honig, B. (1993) On the calculation of pKas in proteins. *Proteins 15*, 252−65.

(26) Schaefer, M., Sommer, M., and Karplus, M. (1997) pH-dependence of protein stability: Absolute electrostatic free energy differences between conformations. *J. Phys. Chem. B 101*, 1663−1683.

(27) Simonson, T., Carlsson, J., and Case, D. A. (2004) Proton binding to proteins: pKa calculations with explicit and implicit solvent models. *J. Am. Chem. Soc. 126*, 4167−4180.

(28) Riccardi, D., Schaefer, P., and Cui, Q. (2005) pKa calculations in solution and proteins with QM/MM free energy perturbation simulations: a quantitative test of QM/MM protocols. *J. Phys. Chem. B 109*, 17715−17733.

(29) Zheng, L., Chen, M., and Yang, W. (2008) Random walk in orthogonal space to achieve efficient free-energy simulation of complex systems. *Proc. Natl. Acad. Sci. U.S.A. 105*, 20227−20232.

(30) Khandogin, J., and Brooks, C. L. (2005) Constant pH molecular dynamics with proton tautomerism. *Biophys. J. 89*, 141−157.

(31) Arthur, E. J., Yesselman, J. D., and Brooks, C. L. (2011) Predicting extreme pKa shifts in staphylococcal nuclease mutants with constant pH molecular dynamics. *Proteins 79*, 3276−3286.

(32) Zhang, B. W., Brunetti, L., and Brooks, C. L., III (2011) Probing pH-dependent dissociation of HdeA dimers. *J. Am. Chem. Soc. 133*, 19393−19398.

(33) Matthew, J. B., Gurd, F. R. N., Garcia-Moreno, B. E., Flanagan, M. A., March, K. L., and Shire, S. J. (1985) pH-dependent processes in protein. *Crit. Rev. Biochem. Mol. Biol. 18*, 91−197.

(34) Sommers, M. *Electrostatic modeling of biological macromolecules in solution*; Ph.D. thesis; Harvard University, 1995.

(35) Vriend, G. (1990) WHAT IF: A molecular modeling and drug design program. *J. Mol. Graphics Modell. 8*, 52−56.

(36) Bashford, D., and Karplus, M. (1991) Multiple-site titration curves of proteins - an analysis of exact and approximate methods for their calculation. *J. Phys. Chem. 95*, 9556−9561.
(37) Tanokura, M., Tasumi, M., and Miyazawa, T. (1976) 1H Nuclear magnetic resonance studies of histidine-containing di- and tripeptides. Estimation of the effects of charged groups on the pKa value of the imidazole ring. *Biopolymers 15*, 393−401.
(38) Bash, P. A., Field, M. J., Davenport, R. C., Petsko, G. A., Ringe, D., and Karplus, M. (1991) Computer-simulation and analysis of the reaction pathway of triosephosphate isomerase. *Biochemistry 30*, 5826−5832.
(39) Cui, Q., and Karplus, M. (2002) Quantum mechanics/molecular mechanics studies of triosephosphate isomerase-catalyzed reactions: Effect of geometry and tunneling on proton-transfer rate constants. *J. Am. Chem. Soc. 124*, 3093−3124.
(40) Brooks, B. R., Bruccoleri, R. E., Olafson, B. D., States, D. J., Swaminathan, S., and Karplus, M. (1983) CHARMM- a program for macromolecular energy, minimization, and dynamics calculations. *J. Comput. Chem. 4*, 187−217.
(41) Chu, J. W., Trout, B. L., and Brooks, B. R. (2003) A super-linear minimization scheme for the nudged elastic band method. *J. Chem. Phys. 119*, 12708−12717.
(42) Brooks, B. R., et al. (2009) CHARMM: the biomolecular simulation program. *J. Comput. Chem. 30*, 1545−1614.
(43) Davis, M. E., Madura, J. D., Luty, B. A., and McCammon, J. A. (1991) UHBD 4.1. *Comput. Phys. Commun. 62*, 187.
(44) Beroza, P., Fredkin, D. R., Okamura, M. Y., and Feher, G. (1991) Protonation of interacting residues in a protein by a Monte Carlo method: application to lysozyme and the photosynthetic reaction center of Rhodobacter sphaeroides. *Proc. Natl. Acad. Sci. U.S.A. 88*, 5804−5808.
(45) Park, S.-Y., Yokoyama, T., Shibayama, N., Shiro, Y., and Tame, J. R. (2006) 1.25 Å resolution crystal structures of human haemoglobin in the oxy, deoxy and carbonmonoxy forms. *J. Mol. Biol. 360*, 690−701.
(46) Shaanan, B. (1983) Structure of human oxyhaemoglobin at 2.1 Å resolution resolution. *J. Mol. Biol. 171*, 31−59.
(47) Silva, M., Rogers, P., and Arnone, A. (1992) A third quaternary structure of human hemoglobin a at 1.7Å resolution. *J. Biol. Chem. 267*, 17248−17256.
(48) Safo, M., and Abraham, D. (2005) The enigma of the liganded hemoglobin end state: a novel quaternary structure of human carbonmonoxy hemoglobin. *Biochemistry 44*, 8347−8359.
(49) Caves, L. S. D., Evanseck, J. D., and Karplus, M. (1998) Locally accessible conformations of proteins: Multiple molecular dynamics simulations of crambin. *Protein Sci. 7*, 649−666.
(50) Kilmarti, J. V., and Rossi-Bernardi, L. (1973) Interaction of hemoglobin with hydrogen-ions, carbon-dioxide, and organic phosphates. *Physiol. Rev. 53*, 836−890.
(51) Rao, M. J., and Acharya, A. S. (1992) Contribution of the gamma-carboxyl group of Glu43(beta) to the alkaline Bohr effect of hemoglobin A. *Biochemistry 31*, 7231−7236.
(52) Simonson, T., Archontis, G., and Karplus, M. (2002) Free energy simulations come of age: Protein-ligand recognition. *Acc. Chem. Res. 35*, 430−437.
(53) Baker, N., Sept, D., Joseph, S., and Holst, M. J. (2001) Electrostatics of nanosystems: application to microtubules and the ribosome. *Proc. Natl. Acad. Sci. U.S.A. 98*, 10037−10041.
(54) Schaefer, M., and Karplus, M. (1996) A comprehensive analytical treatment of continuum electrostatics. *J. Phys. Chem. 100*, 1578−1599.
(55) Schaefer, M., Bartels, C., and Karplus, M. (1998) Solution conformations and thermodynamics of structured peptides: Molecular dynamics simulation with an implicit solvation model. *J. Mol. Biol. 284*, 835−848.
(56) Fermi, G., Perutz, M., Shaanan, B., and Fourme, R. (1984) The crystal structure of human deoxyhaemoglobin at 1.74 Å resolution. *J. Mol. Biol. 175*, 159−174.
(57) Kavanaugh, J., Moo-Penn, W., and Arnone, A. (1993) Accommodation of insertions in helices: the mutation in hemoglobin Catonsville (Pro 37 alpha-Glu-Thr 38 alpha) generates a 3(10)->alpha bulge. *Biochemistry 32*, 2509−2513.
(58) Chan, N., Kavanaugh, J., Rogers, P., and Arnone, A. (2004) Crystallographic analysis of the interaction of nitric oxide with quaternary-T human hemoglobin. *Biochemistry 43*, 118−132.
(59) Kavanaugh, J., Rogers, P., and Arnone, A. (2005) Crystallographic evidence for a new ensemble of ligand-induced allosteric transitions in hemoglobin: the T-to-T(high) quaternary transitions. *Biochemistry 44*, 6101−6121.